AFRL-RV-PS-
TR-2022-0088

SMALL SATELLITE POSITION, NAVIGATION, AND TIMING INNOVATIONS VOLUME II - CONTACT CSAC EXPERIMENT FOR MAXWELL CUBESAT

Mikela Dobbin and Penina Axelrad

University of Colorado Boulder
Aerospace Engineering Sciences, CCAR
3775 Discovery Drive
Boulder, CO 80303

30 August 2022

Final Report

AIR FORCE RESEARCH LABORATORY
Space Vehicles Directorate
3550 Aberdeen Ave SE
AIR FORCE MATERIEL COMMAND
KIRTLAND AIR FORCE BASE, NM 87117-5776

DTIC COPY

NOTICE AND SIGNATURE PAGE

AFRL-RV-PS-TR-2022-0088 HAS BEEN REVIEWED AND IS APPROVED FOR PUBLICATION IN ACCORDANCE WITH ASSIGNED DISTRIBUTION STATEMENT.

//SIGNED//	//SIGNED//
_____	_____
Dr. Spencer E. Olson	Mark E. Roverse, Chief
Program Manager/AFRL/RVB	AFRL Geospace Technologies Division

REPORT DOCUMENTATION PAGE

Form Approved
OMB No. 0704-0188

1. REPORT DATE *(DD-MM-YYYY)*	**2. REPORT TYPE**	**3. DATES COVERED** *(From - To)*
30-08-2022	Final Report	4 Dec 2018 – 30 Aug 2022

4. TITLE AND SUBTITLE
Small Satellite Position, Navigation, and Timing Innovations
Vol. II – CSAC Experiment for MAXWELL CubeSat

5a. CONTRACT NUMBER
FA9453-19-1-0076

5b. GRANT NUMBER

5c. PROGRAM ELEMENT NUMBER
63401F

6. AUTHOR(S)
Mikaela Dobbin and Penina Axelrad

5d. PROJECT NUMBER
3682

5e. TASK NUMBER
EF134353

5f. WORK UNIT NUMBER
V1NE

7. PERFORMING ORGANIZATION NAME(S) AND ADDRESS(ES)
University of Colorado Boulder
Aerospace Engineering Sciences, CCAR
3775 Discovery Drive
Boulder, CO 80303

8. PERFORMING ORGANIZATION REPORT NUMBER

9. SPONSORING / MONITORING AGENCY NAME(S) AND ADDRESS(ES)
Air Force Research Laboratory
Space Vehicles Directorate
3550 Aberdeen Avenue SE
Kirtland AFB, NM 87117-5776

10. SPONSOR/MONITOR'S ACRONYM(S)
AFRL/RVBYT

11. SPONSOR/MONITOR'S REPORT NUMBER(S)
AFRL-RV-PS-TR-2022-0088

12. DISTRIBUTION / AVAILABILITY STATEMENT
Approved for public release; distribution is unlimited (AFRL-2023-1731 dtd 12 Apr 2023).

13. SUPPLEMENTARY NOTES

14. ABSTRACT
This final report documents the work completed by researchers and students in the Colorado Center for Astrodynamics Research (CCAR) and Smead Aerospace Engineering Sciences at the University of Colorado Boulder, to model and develop technologies and algorithms to advance small space platform positioning, navigation, and timing, with a primary emphasis on timing systems. The report is presented in three volumes. Volume 1 presents the CONTACT software defined radio (SDR) based testbed for measurement and ensembling of low size, weight, and power (SWaP) atomic clocks. Volume 2 describes the development of a CSAC flight experiment to be flown on the MAXWELL UNP-9 CubeSat, expected to be launched in 2023. Volume 3 focuses on modeling and analysis of distributed optical time and frequency transfer across small satellites in a large-scale low Earth orbit (LEO) constellation.

15. SUBJECT TERMS
CSAC performance, CubeSat

16. SECURITY CLASSIFICATION OF:			**17. LIMITATION OF ABSTRACT**	**18. NUMBER OF PAGES**	**19a. NAME OF RESPONSIBLE PERSON**
a. REPORT	**b. ABSTRACT**	**c. THIS PAGE**			Dr. Spencer E Olson
Unclassified	Unclassified	Unclassified	Unlimited	44	**19b. TELEPHONE NUMBER** *(include area code)*

This page is intentionally left blank.

TABLE OF CONTENTS

LIST OF FIGURES

Figure **Page**

LIST OF FIGURES (continued)

Figure **Page**

LIST OF TABLES

Table **Page**

Acknowledgements

The authors gratefully acknowledge the specific contributions to the work described in Volume 2 by team members Cydnee Colpaert, Alex Conrad, Laura Davies, Caroline Dixon, Yashica Khatri, Christopher Krebs, and Luciana Schement.

We acknowledge the valuable advice provided by Dr. Joanna Hinks and her colleagues at AFRL who attended our presentations and gave helpful feedback for moving forward with the project; and by Dr. Robert Lutwak of Microchip regarding the performance and testing of the CSACs. Additionally, we thank Dr. Nicholas Rainville for providing overall project guidance; and Aaron Aboaf, Robert Redfern, Anastasia Muszynski, and Bailey Roker from the MAXWELL Team for their important contributions on the orbital CSAC experiment.

Finally, we want to recognize the hard work of all CONTACT team members shown in the table below, who contributed since this project's inception in Spring 2019.

CONTACT Team Project Participants

Last Name	First Name	Position(s)	Dates
Colpaert	Cydnee	MS Graduate Project Team	8/21-5/22
Conrad	Alex	PhD Student Volunteer	1/20-5/20
Davies	Laura	PhD Student Volunteer	9/21-12/21
Desai	Prayag	Independent Study	8/20-12/20
Dixon	Henry	MS Thesis, MS Research Assistant	1/19-2/21
Dixon	Caroline	Undergraduate Research Assistant	8/20-6/21
Dobbin	Mikaela	MS Graduate Project Team, Research Assistant	8/21-8/22
Dowd	Daniel	MS Graduate Project Team, Independent Study	8/19-12/20
Flood	Christopher	PhD Student Volunteer, Research Assistant	8/19-8/22
Khatri	Yashica	MS Graduate Project Team	8/19-6/20
Krebs	Christopher	Undergraduate Research Assistant	6/21-5/22
LaBarge	Quinn	MS Graduate Project Team	8/20-5/21
Mezich	Andrew	MS Graduate Project Team	1/19-5/19
Morris	Tyler	MS Graduate Project Team	8/19-5/20
Nichols	Alexander	MS Graduate Project Team	1/19-5/19
Pedersen	Christopher	Undergraduate Research Assistant	6/22-8/22
Ramaprasad	Rahul	Independent Study	8/19-12/19
Reynolds	Zachary	MS Graduate Project Team	1/19-5/19
Rybak	Margaret	PhD Student Volunteer	1/19-5/19
Schement	Luciana	MS Graduate Project Team	8/20-5/21
Watkins	William	MS Graduate Project Team	8/21-5/22

1. SUMMARY

This final report documents the work completed by researchers and students in the Colorado Center for Astrodynamics Research (CCAR) and Smead Aerospace Engineering Sciences at the University of Colorado Boulder, to model and develop technologies and algorithms to advance small space platform positioning, navigation, and timing, with a primary emphasis on timing systems. The report is presented in three volumes. Volume 1 presents the CONTACT software defined radio (SDR) based testbed for measurement and ensembling of low size, weight, and power (SWaP) atomic clocks. Volume 2 describes the development of a CSAC flight experiment to be flown on the MAXWELL UNP-9 CubeSat, expected to be launched in 2023. Volume 3 focuses on modeling and analysis of distributed optical time and frequency transfer across small satellites in a large-scale low Earth orbit (LEO) constellation.

This is Volume 2, which covers the development of a CSAC flight experiment to be flown on the MAXWELL UNP-9 CubeSat. As an extension of the Clock Ensemble Testbed, the CONTACT team worked in collaboration with MAXWELL, a CubeSat Project at the University of Colorado Boulder, to develop an experiment to characterize CSAC performance in Low-Earth Orbit (LEO). For the experiment, a CSAC is used as an unsteered external oscillator to the on-board GPS receiver to measure clock performance, which is a well-established technique for testing clocks on the ground. The receiver estimates the clock bias and frequency error to provide insight into the CSAC behavior. The on-orbit experiment is designed to span five days, during which measurements of pseudorange, phase, clock bias, and position are planned to be recorded to the flight computer. Telemetry from the CSAC, including temperature and health status, is also collected, allowing analysis of how thermal variations of the space environment affect the CSAC operation. The recorded data are planned to be downlinked via an experimental X-band radio and antenna and will be used to evaluate the accuracy and stability of the CSAC operating in LEO. This report documents the experiment design and testing that was conducted at the University of Colorado Boulder in preparation for the MAXWELL CubeSat launch.

2. INTRODUCTION

MAXWELL (Multiple Access X-band Wave Experiment Located in LEO) is an AFRL University Nanosat Program 6U CubeSat mission that was designed, and is currently being built and tested, by a graduate student project team at the University of Colorado Boulder [1][2]. The goal of the MAXWELL mission is to demonstrate high-rate RF communications technology on a CubeSat platform for future CubeSat applications. The MAXWELL mission has four primary objectives, two of which are to demonstrate S-band uplink and X-band downlink to/from the spacecraft. The CSAC experiment is one of MAXWELL's secondary objectives. The CONTACT team worked in collaboration with the MAXWELL project as the success of the CSAC mission is dependent on the success of MAXWELL's primary mission objectives. Figure 1 depicts a block diagram of the CSAC experiment configuration, which includes both the ground-based live-sky test configuration and the flight configuration.

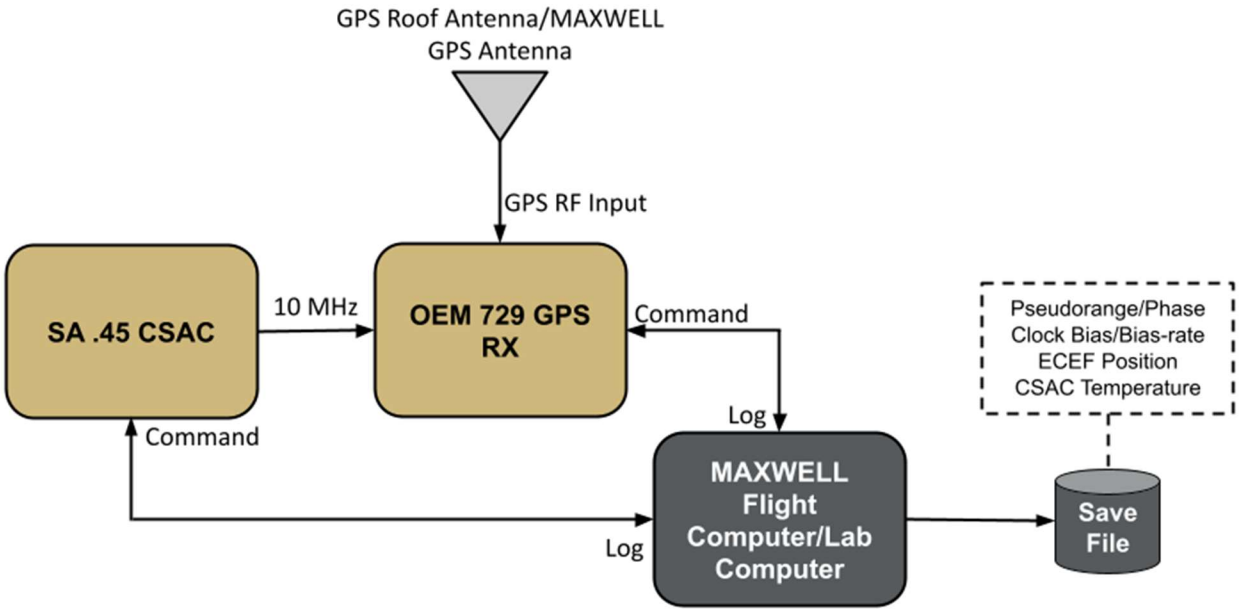

Figure 1. Block diagram of the flight/live-sky test setup for the CSAC experiment

One of MAXWELL's primary mission objectives is to test and demonstrate X-band downlink. This transmitter can downlink data at a rate of 10Mbps [2]. If this demonstration is successful, the X-band system will be used to downlink the CSAC experiment data. In the case that the X-band system is not available for use, MAXWELL can relay a smaller set of CSAC experiment data via a UHF transmitter.

The CSAC flight experiment uses a Microchip SA.45 CSAC [3, 4] and a NovAtel OEM 729 GPS receiver [5]. The CSAC is connected to the receiver as an unsteered external oscillator, enabling observations of the clock performance. The messages from the receiver, which include bias, bias-rate, ECEF position, pseudorange, and phase, are recorded at varying intervals throughout the experiment. The CSAC performance is characterized using the receiver bias and bias-rate solutions. Measurements of pseudorange and phase from the receiver also enable further analysis of the clock's performance in post-processing using NASA JPL's GipsyX software.

Work by the CONTACT team on this flight experiment has been previously presented and reported in references [6, 7, 8].

3. METHODS, ASSUMPTIONS, AND PROCEDURES

In preparation for MAXWELL's hardware delivery, the CONTACT team performed ground testing to provide a baseline for how the CSAC is expected to behave on-orbit. Ground testing is essential for the success of the MAXWELL project and the CSAC experiment as it ensures that the hardware and software interface properly. The flight experiment results will be compared to the baseline performance established with ground testing to understand how the space environment affects the CSAC performance.

The following list summarizes the tests that have been accomplished within our lab facilities.

1. Live-sky testing
2. Thermal chamber testing
3. Magnetic field testing
4. RF/GNSS simulator testing
5. MAXWELL integration & testing

Most of these tests were performed using a NovAtel OEM729 GPS receiver and three Microchip SA.45 CSACs which we identify by the nicknames *Chip*, *Ralphie*, and *Space-Buff*. Live-sky testing is the basis for most of the experiments, with a small number of tests conducted using an RF/GNSS simulator. The NovAtel receiver uses the CSAC as an unsteered external oscillator and is connected to a roof antenna drop (roof drop) atop the Smead Aerospace Engineering Sciences building at CU Boulder to compute GPS measurements as seen in Figure 1. Figure 2 shows the typical lab set-up for performing a live-sky test.

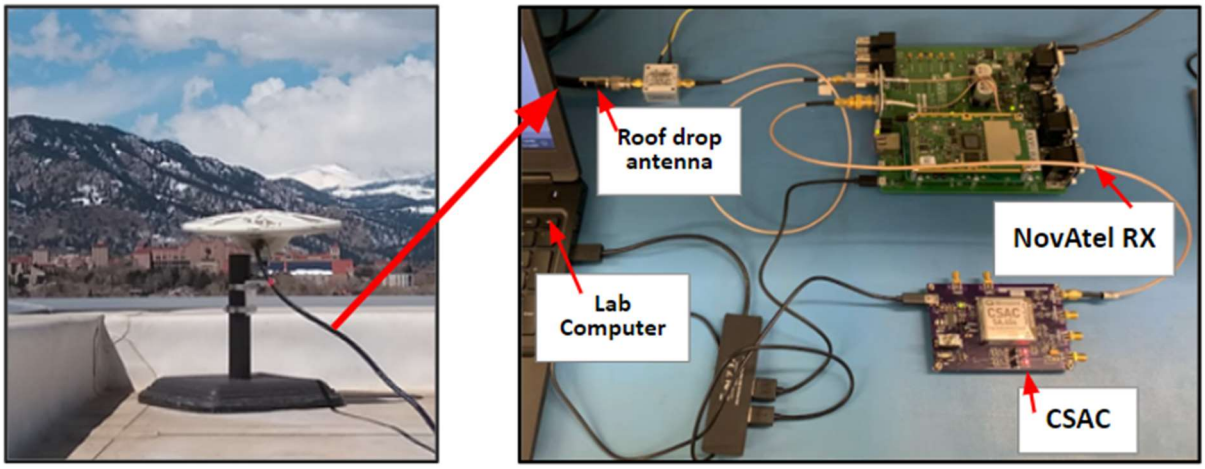

Figure 2. Live-sky test setup

Pseudorange, phase, clock bias, and clock bias-rate are collected from the GPS receiver at a frequency of 1Hz while the telemetry data, including temperature, from the CSACs physics package are also collected at the same rate. Thermal chamber and magnetic field tests were conducted by performing live-sky tests, while placing the CSAC in orbit-like environments. The thermal chamber experiments aim to characterize the CSAC performance under varying temperature profiles. The magnetic field testing provides an understanding of how an increased magnetic field influences the CSAC's performance. The RF/GNSS simulator tests were done to test the performance of the NovAtel OEM719, which unlike the OEM729 is single frequency. This is the same receiver that will be used on-board MAXWELL for the flight experiment, with the primary purpose being to test the receiver in space-like scenarios. The NovAtel receives simulated GPS signals from a Sprient STR4500 simulator. Like live-sky testing, a CSAC is used as an unsteered external oscillator to the GPS receiver.

3.1 Data Analysis Methods

It is important to establish methods that accurately characterize the CSAC's performance, both for ground testing and in preparation for processing the data collected during the MAXWELL

mission. The primary measurements used for characterizing clock performance are the receiver reported clock bias and bias-rate. The time history of clock bias and bias-rate can be used to analyze the environmental influences on clock performance while clock stability can be assessed by computing the Allan Deviations (ADEVs).

3.1.1 Receiver Measurements

The NovAtel OEM729 GPS receiver reports two estimates of the external clock bias and drift — an instantaneous solution and a Kalman filter solution. The Kalman filter can be tuned by inputting h-parameters, but details on the filter implementation are not publicly available [5]. The CONTACT team had previously utilized this Kalman filter as an improved method of CSAC characterization. However, our investigations indicated that the filter appears to be over-smoothing the data. Thus, we rely on the instantaneous solutions for bias and bias-rate to characterize the CSAC behavior.

3.1.2 GipsyX Post-processing

In addition to the bias and bias-rate solutions from the receiver we also consider an advanced method of estimating clock bias and bias-rate through post-processing of GPS pseudorange and carrier phase data. This is done using NASA Jet Propulsion Laboratory software, GipsyX [9], which can be used to produce highly-accurate carrier-phase based estimates of clock bias and bias-rate. Both the instantaneous and carrier-phase estimates of clock bias and bias-rate are used to characterize the CSAC's behavior for ground testing and will be used to analyze the CSAC's on-orbit performance during the MAXWELL mission.

3.1.3. Single Frequency Data Analysis

The receiver used for ground testing has been a dual frequency L1/L2 receiver. However, the receiver chosen for the MAXWELL flight experiment will be a single frequency L1-only receiver. Given that MAXWELL will be in a LEO, at an altitude of nearly 550km, the GPS signals will be somewhat impacted by the ionosphere, but less significantly than those received on the Earth surface. For high precision applications, this would mitigated using a dual frequency receiver, but single frequency operations are common for low-cost CubeSat missions. As such, it was important to identify and evaluate methods to simulate and process the single frequency GPS receiver measurements. We were able to simulate single-frequency measurements in GipsyX by not applying the dual frequency ionospheric corrections. GipsyX outputs the bias and bias-rate measurements using two different methods:

1. C1C and L1C solutions
2. Code only (C1C) solutions

As these measurements are processed from ground-based tests, we would expect to see significant ionospheric errors in comparison to the dual-frequency results. Additionally, the difference between the single and dual-frequency results should be largest during the day when ionospheric activity is highest, thus having a larger contribution to the error in the GPS solutions. Therefore, further post-processing was investigated using a combined C1C/L1C solution to mitigate the ionospheric effects. The GRAPHIC technique is used to combine the code and carrier signals to remove the errors caused by the ionosphere by taking advantage of code-carrier

divergence effect by averaging the code and carrier-phased based results [10]. This is shown in Equation [1].

$$\text{GRAPHIC} = (\text{C1C} + \text{L1C})/2 \quad [1]$$

3.1.4 GipsyX Estimation Limits

The final element of data analysis methods was to identify the estimation limits of GipsyX. This was done by processing GPS observation of a hydrogen maser (H-maser) from the National Institute of Standards and Technology (NIST). In addition, GipsyX results from a receiver observing a Rubidium Frequency Standard atomic clock are given. CSAC dual-frequency GipsyX results were also given. Each dataset was taken from dual-frequency receiver results and processed by GipsyX for a test duration of 24 hours. CSAC and Rubidium data are processed at a 1-Hz rate, and H-maser data was given at a sampling time of 30s.

3.2 Live-sky Testing

Live-sky tests were performed with each of three CSACs named Ralphie, Chip, and SpaceBuff to understand the performance of each clock. The live sky tests were performed using an antenna drop (roof drop) atop the Smead Aerospace Engineering Sciences building at CU Boulder. The roof drop cable was connected to the RF input of a NovAtel OEM729 GPS receiver and the CSAC board was connected to the receiver as an unsteered external clock as shown in Figure 1. Pseudorange, phase, clock bias, and clock bias-rate were collected from the GPS receiver at 1Hz while CSAC temperature and health data were collected from the CSAC physics package at the same rate. The duration of the live-sky tests varied from a few hours to nearly weeklong.

3.2.1 Baseline Clock Characterization Testing

Initial live-sky tests were conducted using the three CSACs and a PRS10 rubidium frequency standard (Rb) to get a baseline for each clock's performance on the ground.

3.2.2 Thermal Testing

A crucial aspect of ground testing for the CSAC flight experiment is understanding the CSAC performance sensitivity to temperature changes. CSAC performance can be influenced by hot and cold temperatures as well as temperature gradients. The three CSACs, Chip, Ralphie, and SpaceBuff, were tested under various temperature profiles to characterize clock performance in a thermal environment like what is expected during the MAXWELL mission. The primary goals were to: determine accurate temperature profiles in LEO, discern the differences in performance each CSAC had for these temperature profiles, and investigate the cause of changes in CSAC performance due to differences in temperature change rate.

Figure 3. Image of CSAC inside of thermal chamber

Constant Temperature Hot Test

A constant temperature hot test was done to get an understanding of how the CSAC is affected by warm temperatures and gain experience using the chamber. The thermal chamber was set to a constant 35ºC, and data were collected for a minimum of 20 hours.

Constant Temperature Cold Test

In order to prepare for the LEO temperature profile test, we conducted a constant temperature cold experiment in the thermal chamber. The purpose of this test was to determine whether condensation developed at the minimum on-orbit internal temperature for MAXWELL. MAXWELL has a heater that turns on when the battery reaches 4ºC; this is approximately the minimum internal temperature for the CubeSat. For this test, no hardware was used; instead, a metal plate was placed inside the chamber during the test. The thermal chamber was set to a constant 4C. After approximately 20 hours, the thermal chamber and metal plate were examined for signs of condensation. A paper towel was used to wipe the inside of the chamber and both sides of the plate to determine whether any condensation was present.

3.2.3 LEO Temperature Profiles

With guidance from Ref [11] and Bret Lamprecht at the CU Boulder Laboratory for Atmospheric and Space Physics, typical LEO temperature profiles were chosen to test CSAC performance. Depending on the satellite hardware, the CSAC on-board MAXWELL can be exposed to temperatures between -10 degrees Celsius and 50 degrees Celsius. However, temperature usually changes by only 20-30ºC within a typical orbit period of 90 minutes. Therefore, an average rate of temperature changes around 0.25ºC/min can be expected during the mission, with an upper bound of 0.5ºC/min. It should be noted that the anticipated temperature extremes are within the CSAC operational specifications, of -10ºC and 70ºC at rates under 0.5ºC\min [4, 12]. Given that the upper bounds of the potential temperature profiles are at/near the operational limits of the CSAC, it was important to test the CSAC at these bounds.

Four temperature profiles were created to test the CSAC performance. These profiles are detailed in Table 1. Each profile was designed to expose the CSACs to the expected temperature ranges and gradients in LEO. The profiles introduce different ranges, rates of change, and soak times.

Temperature profiles with multiple rates of changes are included to isolate how the rate of change influences CSAC behavior.

Table 1. LEO temperature profiles tested on CSACs

Profile	Temperature Range	Temperature Rates of Change	Profile Characteristics
1	+5°C to +35°C	0.5°C per min	60 min ramp up time and 60 min ramp down time
2	-10°C to +5°C	0.25°C per min 0.5°C per min	60 min ramp up time and 60 min ramp down time 30 min ramp up time and 30 min ramp down time
3	0°C to +20°C	0.33°C per min 0.22°C per min	60 min ramp up time and 90 min ramp down time 90 min soak at 20°C
4	+35°C to +50°C	0.25°C per min 0.5°C per min	60 min ramp up time and 60 min ramp down time 30 min ramp up time and 30 min ramp down time 60 min and 30 min soak at 20°C

Each CSAC has a unique response to the temperature changes. During each test, the CSAC telemetry parameters were recorded. These parameters include the clock status, temperature, heater power, and the tuning voltage applied to the temperature compensated crystal oscillator (TCXO) which aims to keep the clock stable. While heater power response to temperature changes was consistent among all three CSACs, each clock exhibited differing TCXO tuning voltage response. However, correlation between temperature, tuning voltage, and heater power was seen for all three CSACs.

3.2.4 CSAC Temperature Calibration

Before shipping the CSACs off to users, Microchip calibrates each CSAC to empirically determine and set the thermal constants for temperature compensation in the presence of thermal variations. The quality of the clock and the calibration drives the clock response to temperature changes. Microchip, the CSAC's manufacturer, tests the CSACs on a temperature profile that includes multiple soaks at 10ºC increments [12]. An example of this test is shown in Figure 4. When no compensation is applied, the CSAC frequency offset is expected to increase/decrease in response to the changing temperature. However, if tuned correctly, the frequency offset should be distributed about zero with little indication of temperature change. To evaluate the CSAC temperature compensation of our CSACs in comparison to that reported by Microchip in Figure 4, we tested our CSACs under a similar profile.

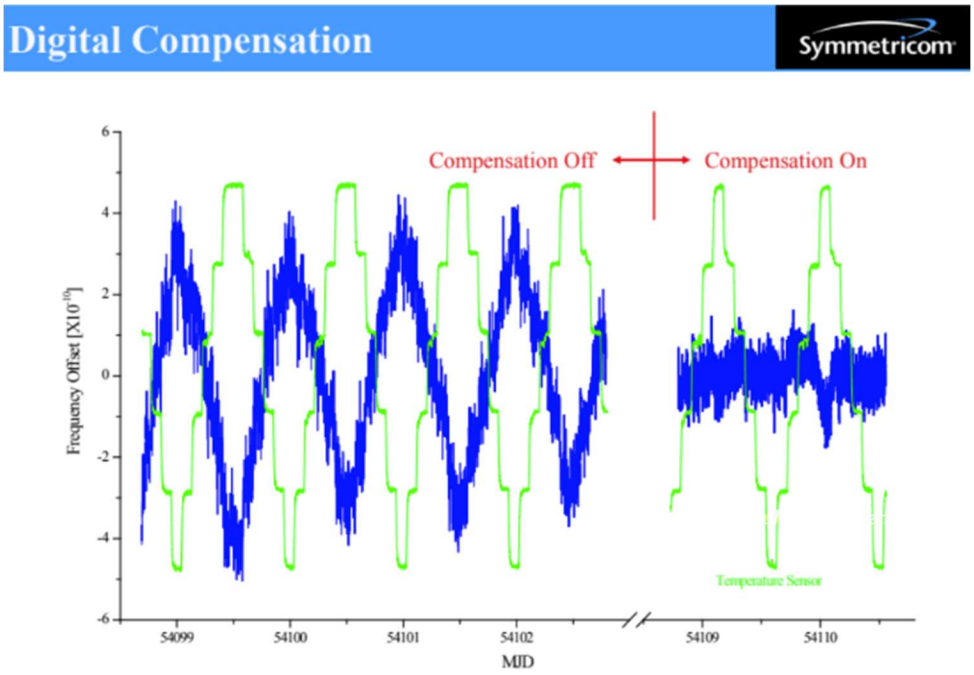

Figure 4. MicroChip temperature tuning experiment [from 12]

3.2.5 Magnetic Field Testing

The influence of magnetic field is another concern for on-orbit operations. MAXWELL will use three orthogonal torque rods to assist with spacecraft attitude control and reaction wheel momentum dumping. The current configuration of MAXWELL has the CSAC approximately 7 cm away from the closest torque rod. By design, torque rods generate an electromagnetic field while in use. The CSAC user manual reports that the CSAC is sensitive to magnetic fields up to 2 Gauss and additional testing by the CSAC manufacturer, MicroChip, reports that the CSAC can be damaged in magnetic fields greater the 10 Gauss [3]. The purpose of our magnetic testing is to identify the worst-case scenario of the magnetic field of the MAXWELL torque rod, determine whether the CSAC is at risk of being damaged, and characterize the CSAC's sensitivity to a changing magnetic field.

To determine the magnitude of the magnetic field generated by the torque rods, the three torque rods were assembled in the same configuration as what will be seen for MAXWELL. A Samsung Galaxy S6 smart phone magnetometer was placed where the CSAC will be located on board to measure the magnetic field. This configuration is shown in Figure 5.

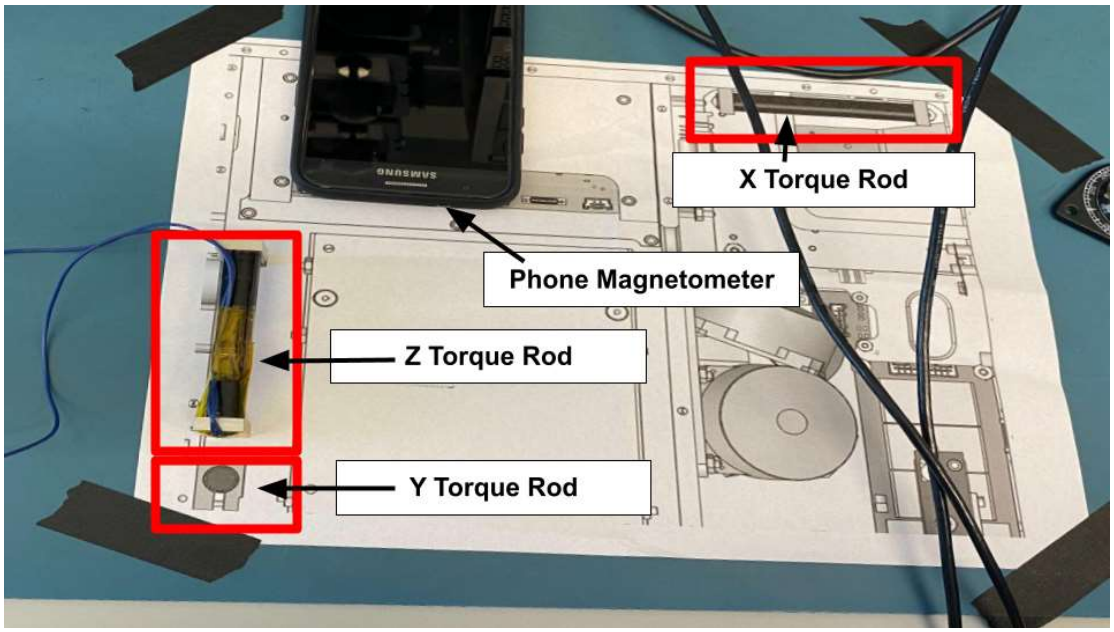

Figure 5. MAXWELL torque rod and phone set up on to-scale MAXWELL printout

Each torque rod was powered from 0 to 5V twice, once with current towards the phone or upwards for the vertical torque rod, and then with the current flowing the opposite direction. The resulting magnetic field was recorded using the phone magnetometer. We were able to verify the accuracy of the phone magnetometer by comparing the measured magnetic field to the magnetic field in Boulder as reported by National Oceanic and Atmospheric Administration (NOAA).

Once field strength was established, we moved to testing the clocks in the B-field. Microsemi reports that the CSAC can experience frequency changes of ±9E-11/Gauss in magnetic fields that are less than 2 Gauss [12]. The CSAC was tested with the Z torque rod, which produced the largest B-Field in the individual torque rod testing as shown in Figure 5. The testing set up with the CSAC is displayed in Figure 6.

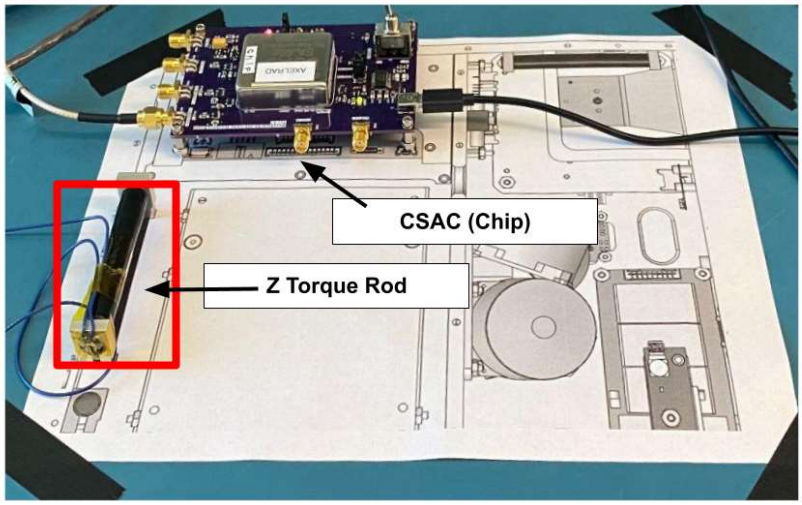

Figure 6. Torque rod and CSAC setup on to-scale MAXWELL printout

The CSAC is connected to the NovAtel OEM 729 receiver as an unsteered external oscillator and a live-sky test is performed using a roof drop cable. While the CSAC is powered and collecting data, the Z torque rod cycles between 0 and 5V roughly every 10 minutes. Given that measured magnetic field at 5V from the torque rod is roughly 0.8 Gauss, we expected to see a visible frequency change with an applied magnetic field over the course of 10 minutes. This test was performed twice (on separate days).

3.3 RF/GNSS Simulator Testing

3.3.1 Locked-Clock Testing

To prepare for GPS operation in LEO, it is common to use and RF simulator to create signal representable of what the receiver will see at high velocities from orbital motion. The first step in simulator testing for the clock experiment is to determine whether the simulator can lock to an external reference. For the RF/GNSS simulator locked-clock test, a Spirent STR4500 simulator was connected to the MAXWELL engineering development (EDU) receiver through the antenna port on a NovAtel development board. The MAXWELL EDU receiver is a single frequency NovAtel OEM719 receiver. The CSAC SpaceBuff was connected to the receiver as an unsteered external oscillator via the development board. SpaceBuff was also connected to the Spirent simulator as an external reference. The test setup is shown in Figure 7. In this test, since the reference clock for both the simulator and the receiver are the same, the clock bias should be zero.

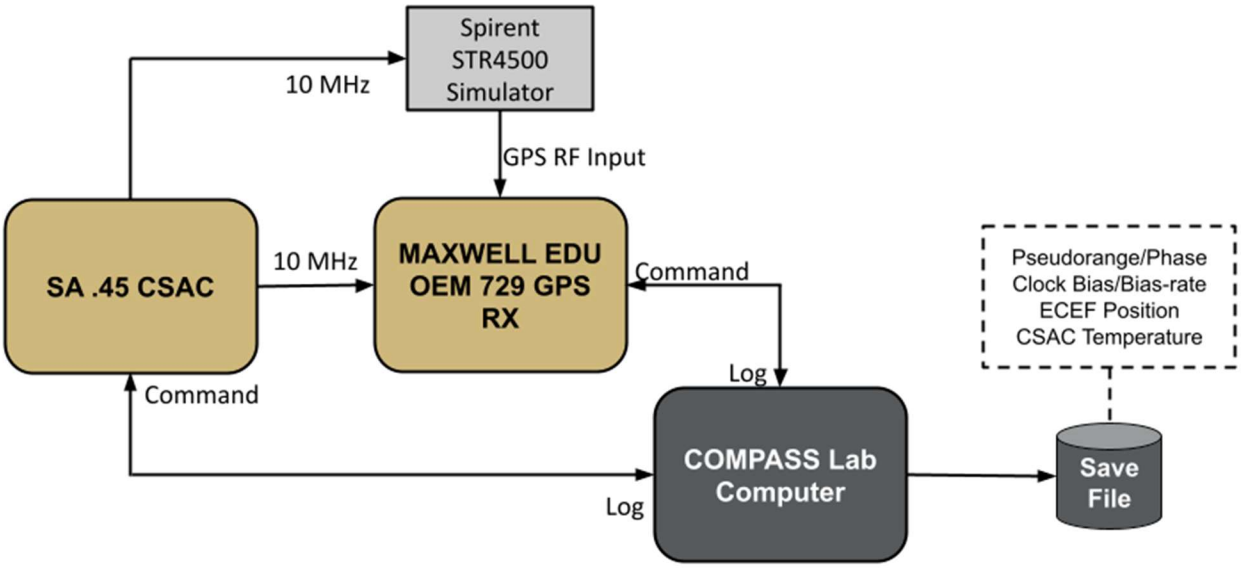

Figure 7. Locked-clock testing setup using CSAC as external reference to GPS receiver and Spirent simulator

3.3.2 Flight Mode Testing

The success of the locked clock tests allowed the team to move on to testing in flight mode. Flight mode testing connects the Spirent simulator to the EDU receiver through the antenna port on the NovAtel development board. The Rb is used as an external reference to the simulator while the CSAC is an unsteered external reference to the EDU receiver. This setup is labeled flight mode because it is comparable to the setup that will be used on-orbit. Figure 8 shows the block diagram of the flight mode test.

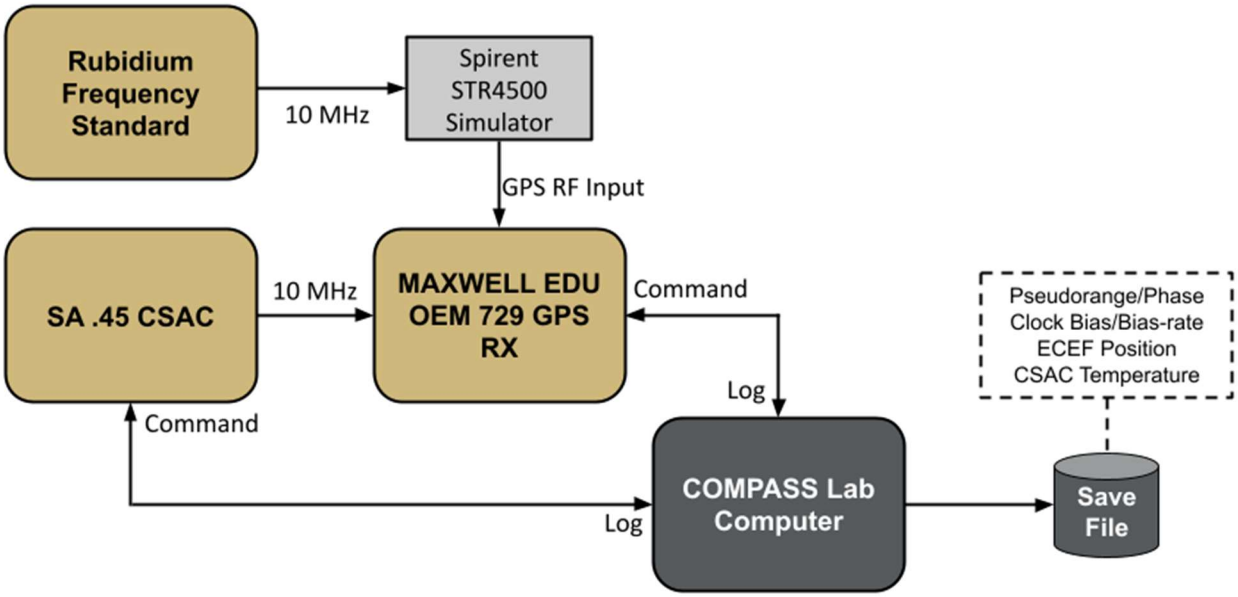

Figure 8. Flight mode testing setup using CSAC as external reference to GPS receiver and Rb as external reference to Spirent simulator

A flight mode test was conducted using the Ralphie CSAC and the same simulation that was used for the locked-clock testing. The simulation was a LEO which ran for approximately 3.5 hours.

3.4 MAXWELL Integration & Testing

MAXWELL final hardware delivery has slipped to 2023. As such, the MAXWELL team intends on completing their hardware and software development and testing by end of 2022 or early 2023. In anticipation for MAXWELL's system testing, the CONTACT team focused on three time-independent phases of integration and testing with the MAXWELL team. These three phases are hardware testing, GPS Visibility and Pointing Modes, and Software Integration.

3.4.1 Hardware Testing

Hardware Testing was conducted to test the MAXWELL components to verify that performance is on-par with the COMPASS lab CSACs, receiver, and antenna. This was done to ensure the CSAC experiment goes as expected and is comparable to ground testing so far. Also, each CSAC has its own performance characteristics, and it is paramount that the CSAC performance is tested prior to flight, to identify any characteristic changes it may exhibit while in space. Hardware testing of the MAXWELL components consists of conducting live-sky testing of the Engineering Development Unit (EDU) CSAC, running the flight CSAC in a long duration experiment, testing

the receiver using a COMPASS CSAC (Chip) and a roof drop, and testing the antenna with the COMPASS receiver.

4. RESULTS AND DISCUSSION

4.1 Data Analysis Method Results

4.1.1 Receiver Measurements Results

It was discovered that the filtered and instantaneous bias and bias-rate outputs from the NovAtel OEM729 do not agree. This behavior is depicted in Figure 9 which compares the ADEV for between the Kalman filter and the instantaneous solution. The ADEV results from the filter show unexpectedly good stability in the short term, followed by an unexplained bump between time constants of 10 and 100 seconds. These unusual results from the filter are seen consistently throughout additional live-sky tests, indicating that it is not an accurate representation of CSAC behavior and should not be used to evaluate CSAC performance.

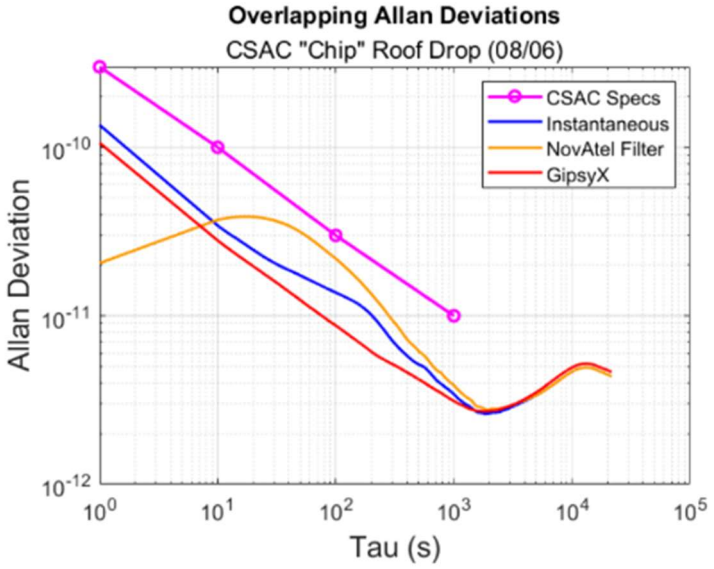

Figure 9. ADEV comparison from Chip live-sky test

4.1.2 GipsyX Post Processing Results

Figure 9 also includes the ADEV computed using the GipsyX carrier-phase estimates of clock bias. Not only do the ADEV results using GipsyX validate the instantaneous solutions, but we also see that the GipsyX solution does not have the bump at a time constant of ~100 seconds. The smaller ADEV with GipsyX at short time constants is expected due to the significant reduction of noise and multipath effects from using the carrier-phase estimates. This reduction of noise is especially visible when comparing the time history of bias-rate, shown in Figure 10, where the overall amplitude of the bias-rate is minimized compared to the instantaneous solutions.

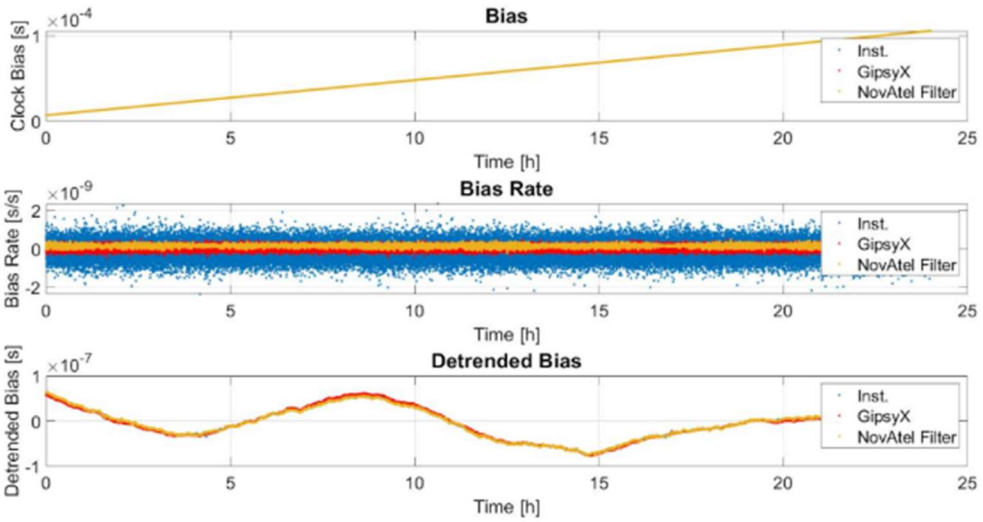

Figure 10. Bias, bias-rate, and detrended bias time history comparison

4.1.3 Single Frequency Data Analysis Results

Figure 11 compares the time-series of the bias, bias-rate, and detrended bias from the various GipsyX solutions methods. We can see that the C1C-only solutions produce the most outliers, which is most obvious when considering the bias-rate. However, further differences between the results are not obvious. For further comparison, Figure 12 reports the OADEV results from the clock bias solutions to compare the clock stability from each solution.

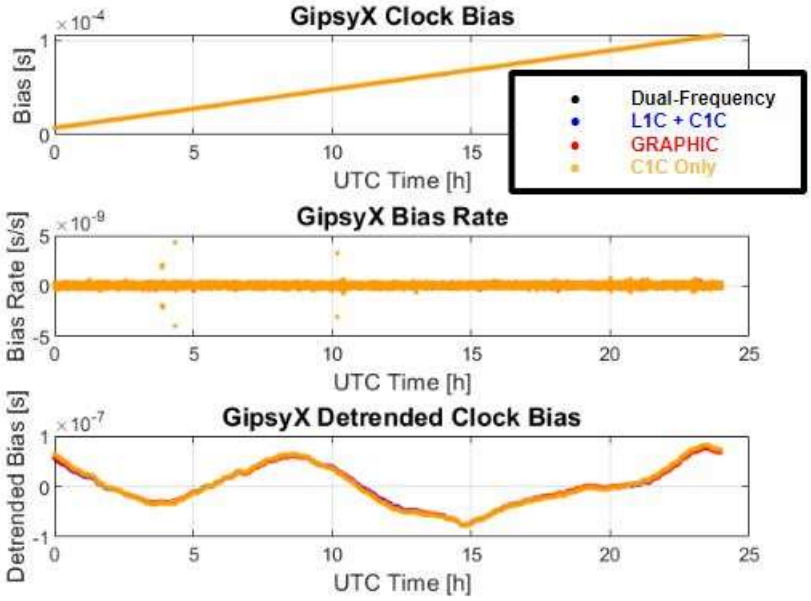

Figure 11. Time history of GipsyX clock solutions for CSAC chip with different measurement types

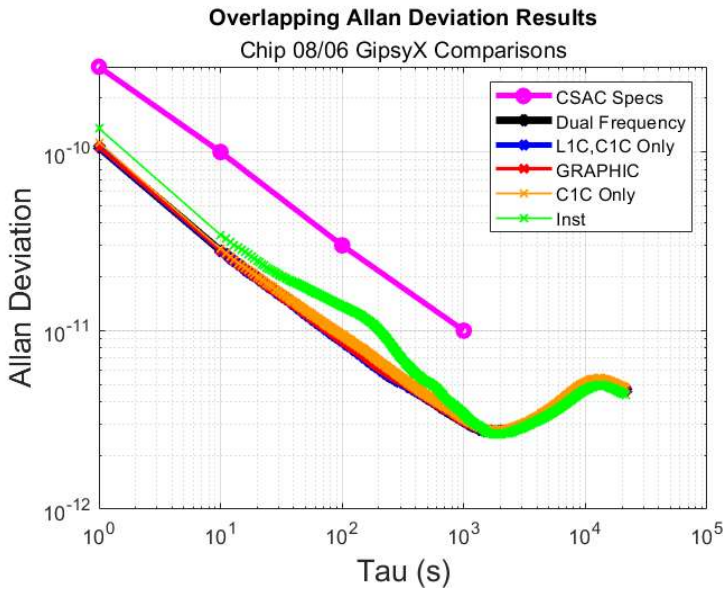

Figure 12. OADEV of dual frequency, L1C + C1C, GRAPHIC, code-only, and instantaneous (inst.) solution from 8/06/21 test with CSAC Chip

In Figure 12, we note at an averaging time of about 100s, there is a "bump" in the instantaneous OADEV which can likely be attributed to multipath. These results prove interesting, because without the carrier-phase based estimation, this multipath effect should not be smoothed. However, the "C1C Only" GipsyX results smooth the bump and align closely to dual-frequency GipsyX results. It was suspected that a static position constraint within GipsyX causes the bump at a time constant of 100 seconds to be smoothed.

To further understand the code-only results from GipsyX, the station position estimation was modified from static-mode to kinematic-mode to remove the possibility of additional smoothing within GipsyX. The purpose of these results was to "un-fix" the receiver location estimation, which could have been inadvertently smoothing the data. Figure 13 compares the kinematic-mode results to the previous outputs. The results show significant difference between the kinematic solution when compared to the previous outputs, notably in the bias-rate outliers and in the detrended clock bias. Figure 14 reports the OADEV with the kinematic results included.

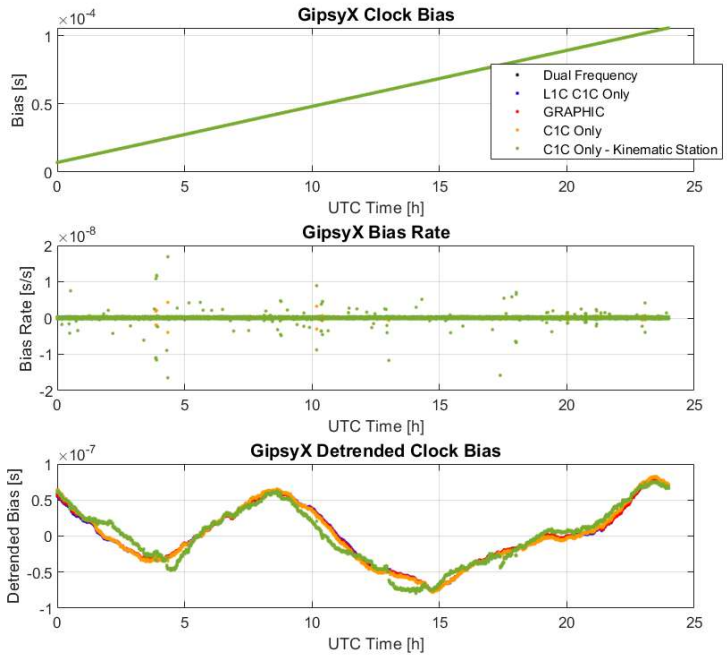

Figure 13. Time series of GipsyX output to compare static and kinematic output modes.

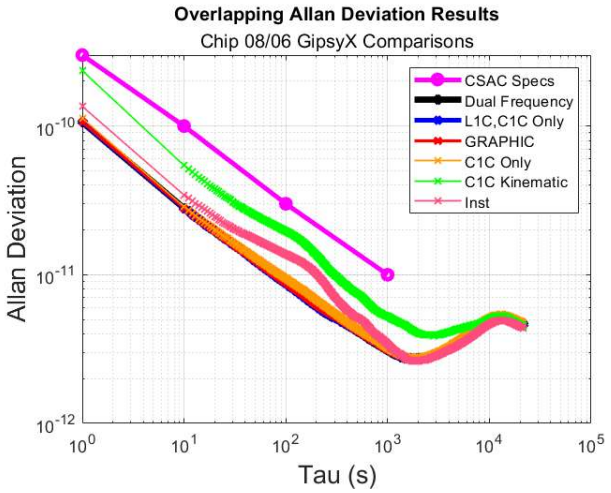

Figure 14. ADEV comparison of GipsyX static and kinematic output modes

The kinematic code only GipsyX now reports a small bump at about a 100s averaging time as well as overall worse stability when compared to the static mode as well as the instantaneous solutions. This is likely because the receiver uses dual-frequency corrections with the code and carrier compared to code-only results using GipsyX. Figure 15 reports the bias differences between each of the single frequency methods (L1C, C1C, and GRAPHIC) and the dual frequency results.

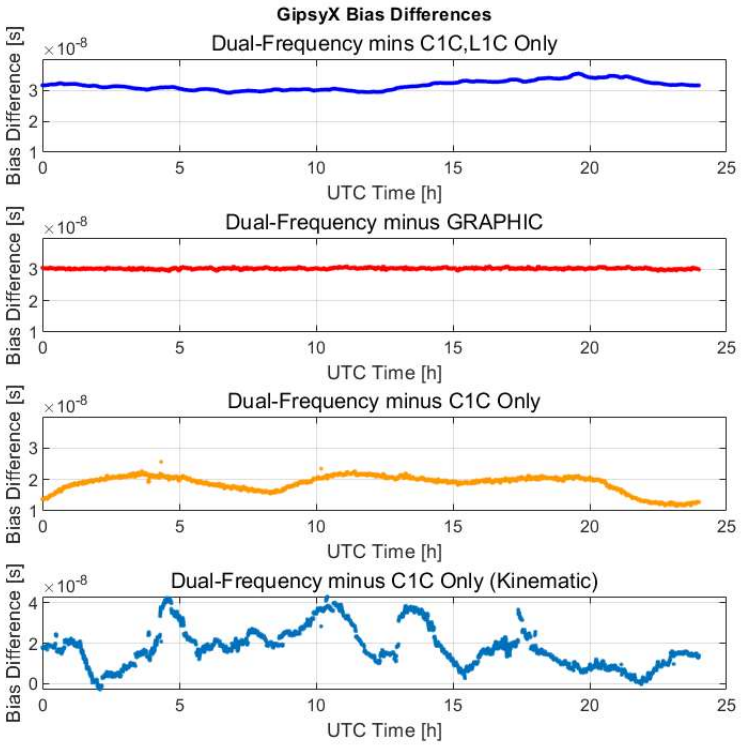

Figure 15. Single frequency solution error with respect to dual frequency solutions

The bias differences from dual-frequency GipsyX shown in Figure 15 are in the order: C1C and L1C only, GRAPHIC, code-only (static-mode), and code-only (kinematic-mode). In the plot comparing C1C and L1C only (top), there is a slight increase in bias difference beginning at about 15:00 UTC time, which corresponds to 10:00 MST (local time of test location). Despite the small scale, this shows that there are increased differences of clock bias in the daytime hours which correspond to higher ionosphere activity and thus, higher errors due to the ionosphere. As predicted, the GRAPHIC results smooth out these ionospheric differences from the C1C+L1C only results. This indicates that the GRAPHIC technique successfully mitigates some of the ionospheric errors. Given that the MAXWELL satellite will face ionospheric effects on a much smaller scale, this gives us confidence that the data obtained from the flight experiment to see an accurate representation of on-orbit CSAC performance. The code-only bias differences given in the third subplot with a static station enabled within GipsyX show a 10-20 nanosecond deviation. When a kinematic station with code-only results is compared to dual-frequency bias in the fourth subplot, these differences are much greater. To further investigate the code-only results, point solutions were taken from the corresponding RINEX GPS file from this test and only C1C broadcast data was processed. Figure 16 and Figure 17 compares the different code-only time series and OADEV results respectively.

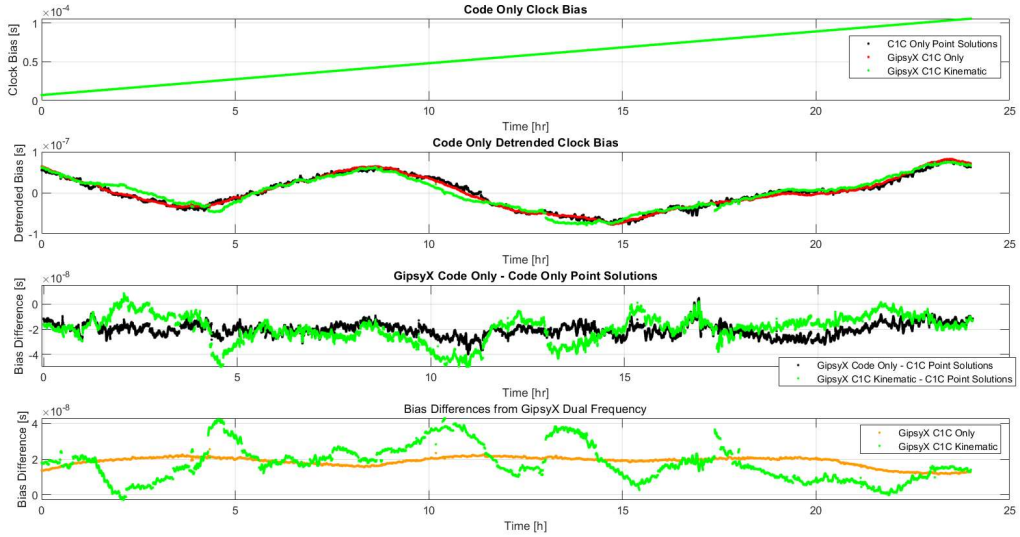

Figure 16: Time series comparison of code-only solutions

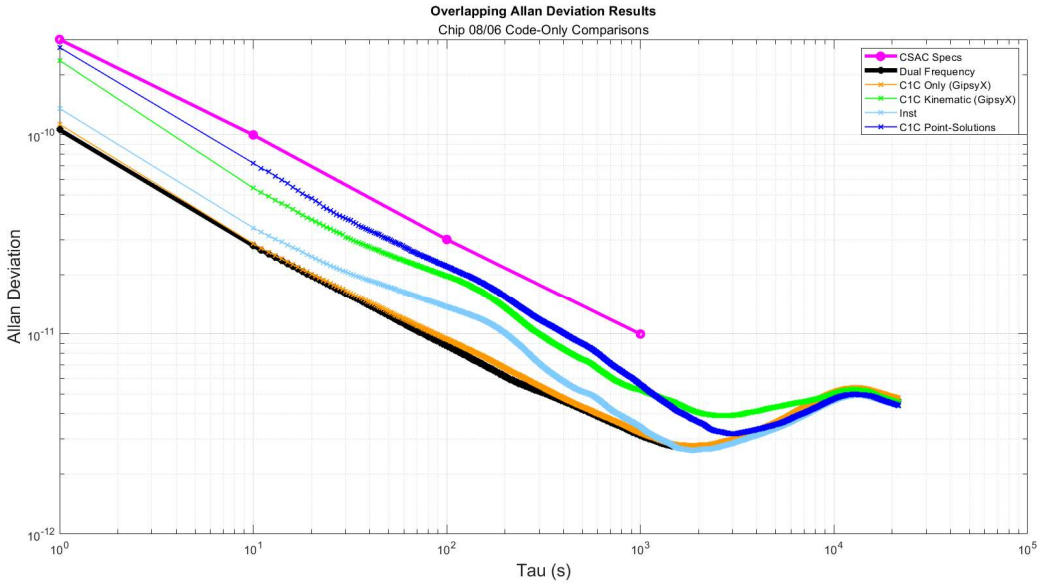

Figure 17. ADEV comparison of code only solutions

As can be seen from Figure 17, the GipsyX kinematic code-only results show improved stability as compared to the code-only point solutions until about a 1000s averaging time. Both results show the same bump at about a 100s averaging time which likely indicates errors due to multipath. This makes sense, as GipsyX uses precise orbit data that is more accurate than the broadcast data used in processing the point solutions. In addition, both results are less stable than the instantaneous dual-frequency laboratory receiver measurements. While investigation of code-only results using GipsyX is still a work in progress, we anticipate that both code and carrier data will be received from the MAXWELL experiment which we have shown to be successful in mitigating the ionospheric errors that typically arise with single-frequency measurements.

4.1.4 GipsyX Estimation Limits Results

GipsyX was used to process GPS observations of two different reference clocks, a Rb and an H-maser for the purpose of characterizing the limits of the software. Figure 18 shows the timeseries comparison and Figure 19 shows the OADEVs of these clocks.

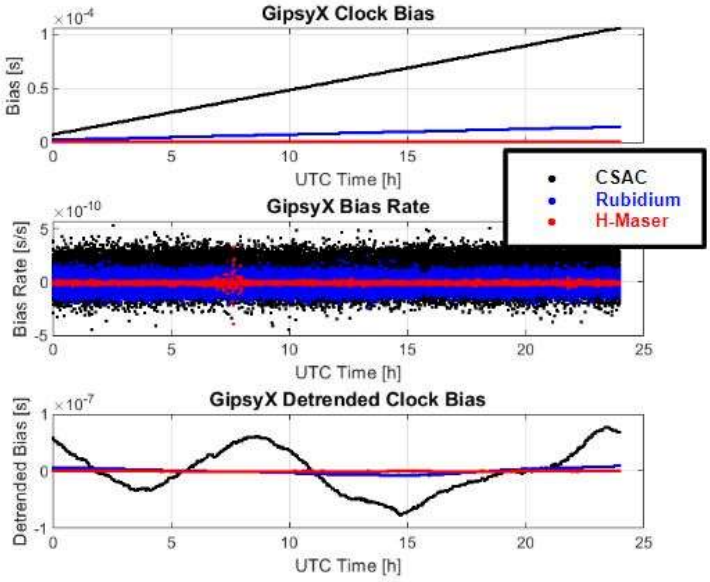

Figure 18. Time series comparison of GipsyX post-processing with Rubidium and H-maser reference clocks

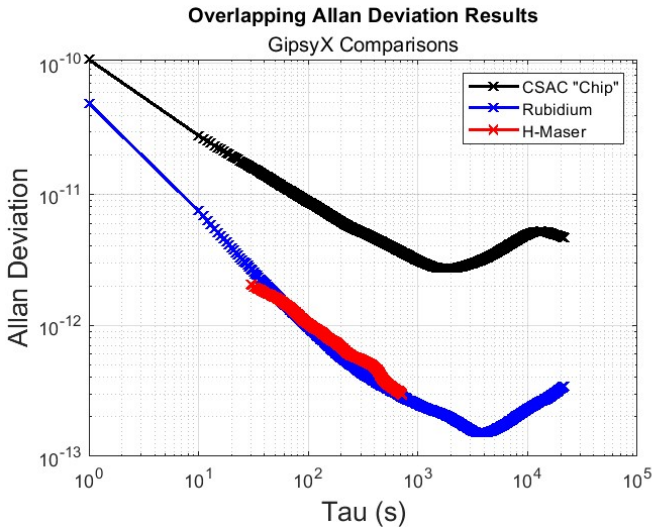

Figure 19. ADEV comparison of GipsyX post-processing with Rubidium and H-maser reference clocks

From the time series results given in Figure 18, we see that the Rb bias-rate has better stability than the CSAC, and the H-maser is improved from that. The most notable result is the significant noise reduction in bias rate from the CSAC to Rubidium to H-maser. From the OADEV results in Figure 19, Rb shows greatly improved stability over a CSAC which is expected. However, H-

masers are more stable than Rubidium atomic clocks, which is not shown in these results. This indicates that the noise in the carrier-phase based clock solution in GipsyX limits our ability to observe the underlying clock behavior at these time scales.

4.2 Live-sky Testing Results

4.2.1 Baseline Clock Characterization Testing Results

The results of the initial live-sky tests with the three CSACs, Chip, Ralphie, and SpaceBuff are shown in Figure 20. The CSACs are listed from most to least stable: Chip, Ralphie, and SpaceBuff. All clocks performed within the CSAC specification [3, 4].

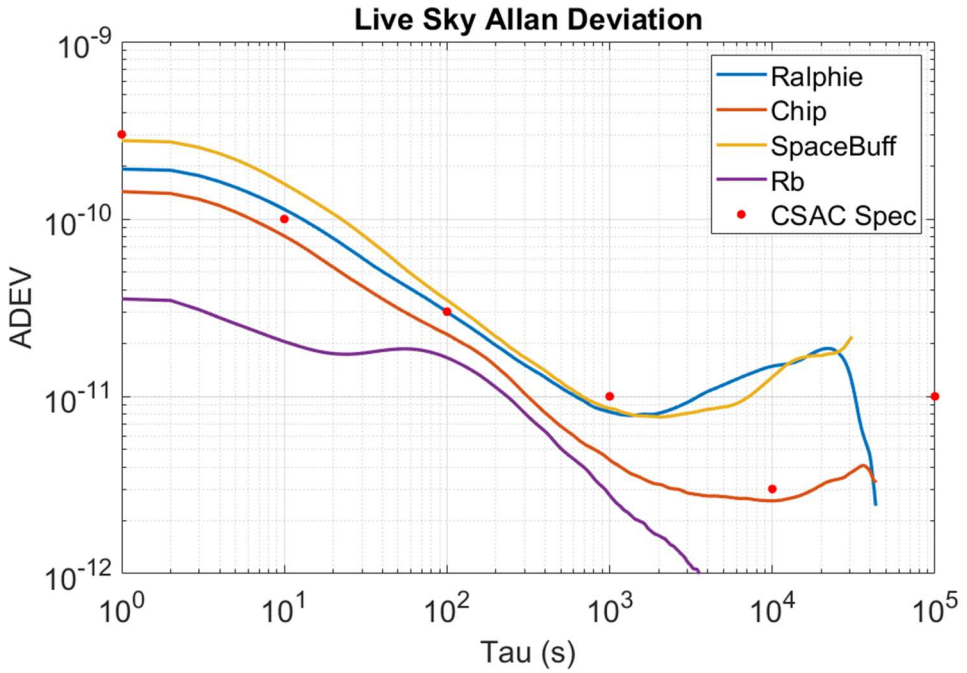

Figure 20. ADEV using receiver estimated clock bias from all three CSACs and Rb from live-sky test

4.2.2 Constant Temperature Thermal Testing Results

Constant Temperature Hot Test Results

The CSAC did not demonstrate any loss of performance when soaked at an elevated temperature. In fact, Ralphie performed slightly better than expected during the thermal test. The resulting ADEV can be seen in Figure 21. This ADEV behaves very close to the CSAC specifications. It is unclear as to why Ralphie performed slightly better than expected in the thermal chamber hot test.

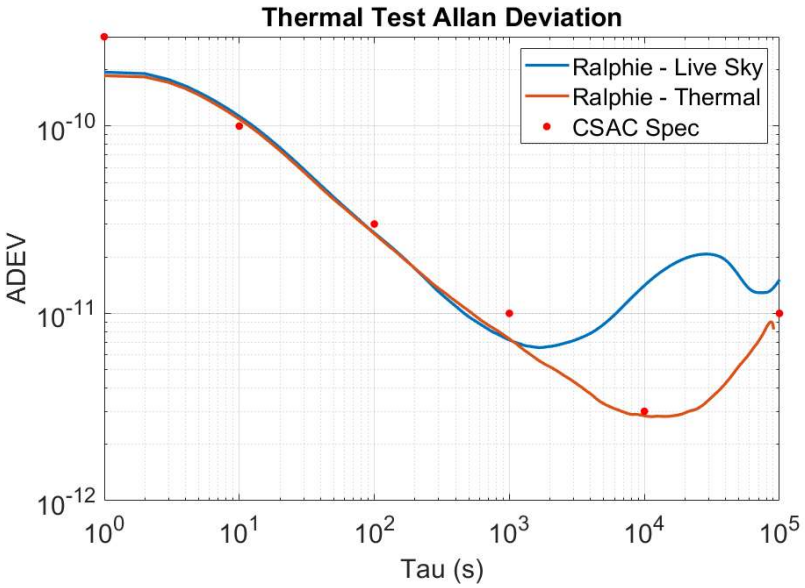

Figure 21. ADEV using receiver estimated clock bias of Ralphie in live-sky and constant temperature hot tests

In addition to the ADEV plot, the receiver estimated clock biases were detrended and plotted versus time in Figure 22. The plot shows that the live sky test has a slow, 12-hour sinusoidal trend over time while the thermal tests remain relatively constant. This difference in the bias over time corresponds to the difference in the ADEV. It is suspected this trend is due to minor temperature oscillations within the lab that the live-sky test is performed.

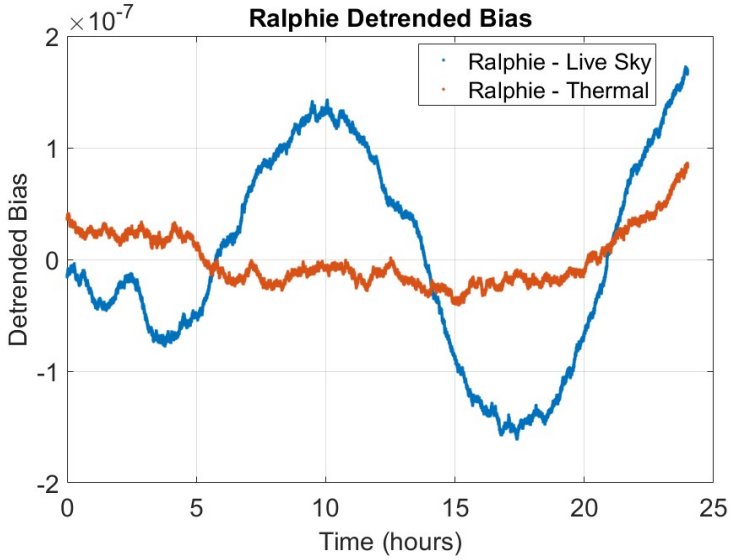

Figure 22. Detrended clock bias of Ralphie comparing live-sky and constant temperature hot test

Constant Temperature Cold Test Results

No condensation appeared in the chamber or on the metal plate.

4.2.3 LEO Temperature Profile Results

LEO Temperature Profile 1

The purpose of performing Temperature Profile 1 was to characterize clock stability while experiencing temperature changes. Ralphie and SpaceBuff were tested under a temperature profile which reflects the upper boundary of what the CSAC is expected to experience in LEO. Figure 23 depicts the ADEV from both clocks compared with the ADEV from a live-sky test with no temperature variation. This comparison indicates that heating and cooling in the thermal chamber effects clock stability, however further analysis is required to characterize the specific effects of temperature on clock stability.

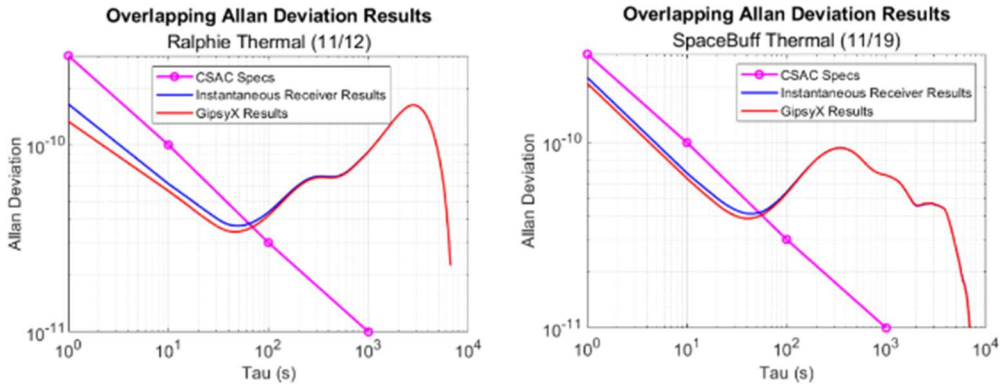

Figure 23. ADEV from temperature profile 1, Ralphie (left) and SpaceBuff (right)

LEO Temperature Profile 2

To better understand the role temperature rate of change plays in clock performance, all three CSACs, Chip, Ralphie, and SpaceBuff, were tested in a 7-hour temperature profile that uses two rates of change within the same temperature range. It is important to note that there are gaps in CSAC telemetry from SpaceBuff during this test that are suspected to be due to an unstable serial port connection. Nevertheless, the results from this test are included because the estimated clock bias and drift from the receiver are intact. Figure 24 compares each CSAC's heater power and tuning voltage response during this test. As expected, heater power is inversely related to changes in temperature. Each plot displays a clear relationship between tuning voltage and temperature changes, although the voltage step size and dwell time at each voltage level vary between the clocks. Both the heater power and tuning voltage parameters show that SpaceBuff is offset from Chip and Ralphie. Without additional testing, it is unclear if this is due in part to the gaps in data or if it is an inherent characteristic of SpaceBuff.

Just as each CSAC responds to changes in temperature, as seen in Figure 24, we look to Figure 25 to highlight how temperature affects clock frequency. Once again, the gaps in SpaceBuff's temperature data are likely due to an unstable serial port connection but do not necessarily result in any degradation of its performance. Shifts in the detrended clock bias for all three clocks align with changes in the chamber temperature. The CSAC data sheet reports that rates of 0.5ºC/min are at the limit of the recommended operation resulting in frequency change up to ±5E-10. Unexpectedly, the amplitude of the peaks in the detrended clock bias for all three clocks are reduced during the faster rate of temperature change.

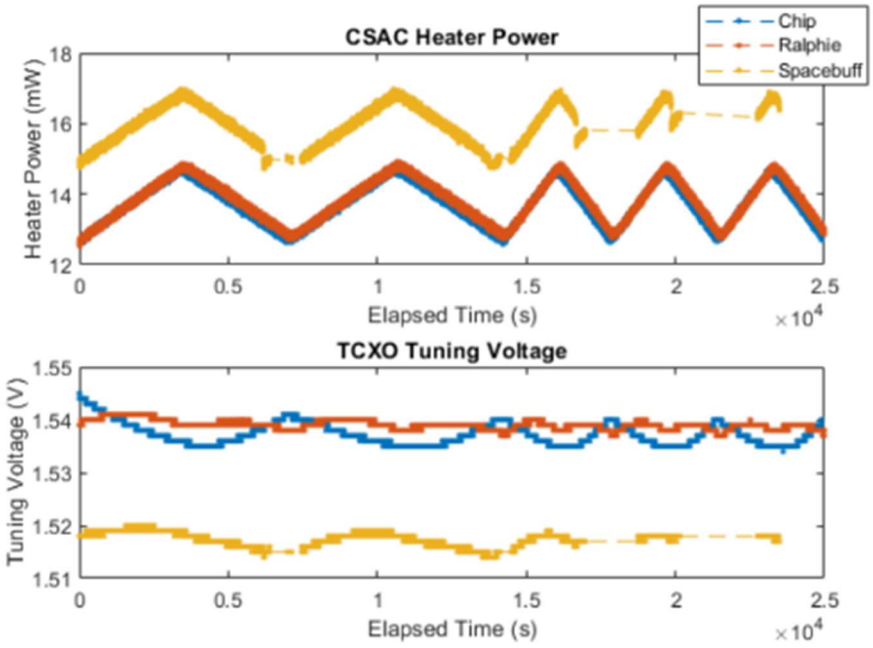

Figure 24. Chip, Ralphie, and SpaceBuff comparison of heater power and tuning voltage over time from Temperature Profile 2

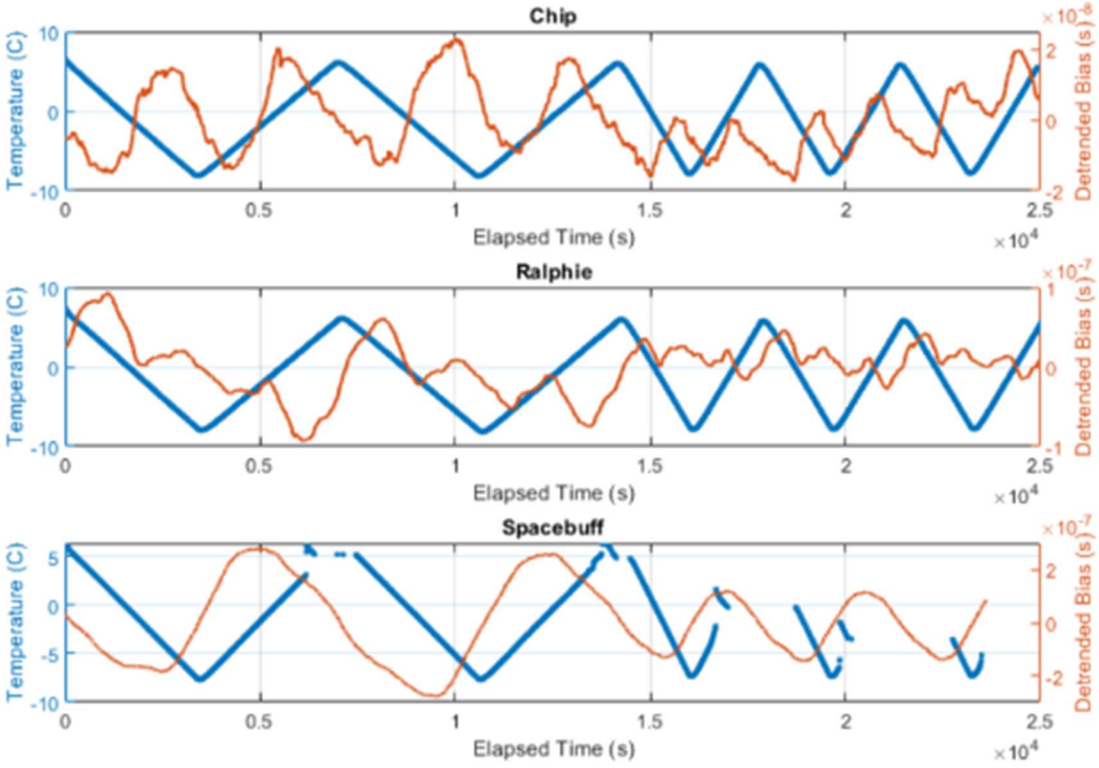

Figure 25. Chip, Ralphie, and SpaceBuff comparison of detrended bias and temperature over time from Temperature Profile 2

The clocks exhibit distinctly different tuning voltage characteristics. The purpose of tuning voltage adjustments is to account for the temperature sensitivity of the TCXO within the CSAC module. Therefore, any lack of compensation for temperature could influence the clock performance. The results from this test reinforce that each clock has a unique response to temperature changes and that there is an overall correlation between changes in temperature and clock performance. For additional comparison, each clock's bias, bias rate, and detrended bias have been plotted together in Figure 26. The detrended clock bias curve brings attention to the impressive stability of Chip over time as it exemplifies the smallest variation in frequency among all the clocks.

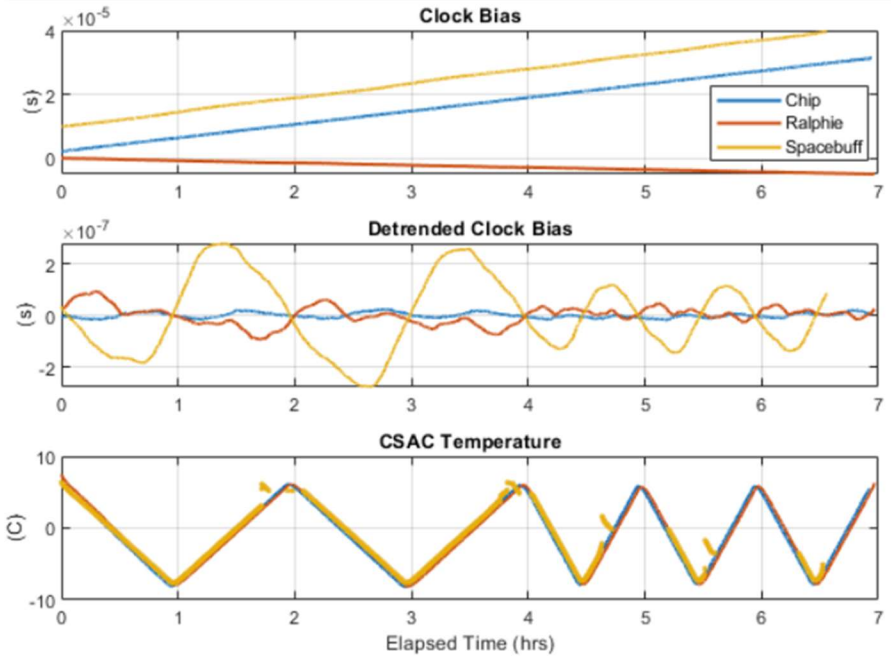

Figure 26. Chip, Ralphie, and SpaceBuff clock bias, detrended bias, and temperature comparison from Temperature Profile 2

LEO Temperature Profile 3

The CSACs were also tested with temperature profiles that include thermal soaks in order to further investigate the clock response to temperature changes. It was found that the detrended clock bias trends linearly during soak periods as opposed to the cyclical behavior that is seen during ramp times. This suggests that in the absence of temperature changes to respond to, the CSAC is quite constant over this time scale. This behavior was discovered during a test using SpaceBuff shown in Figure 27. During the 90-minute soak period, the detrended clock bias strays away from the cyclical pattern, and linearly decreases. Once the temperature began to change again, the detrended clock bias reverted to the behavior seen prior to the soak. Notably, the CSAC controller can be seen responding to changes in temperature by the alignment of detrended bias, heater power, and tuning voltage overlaid with the clock's temperature.

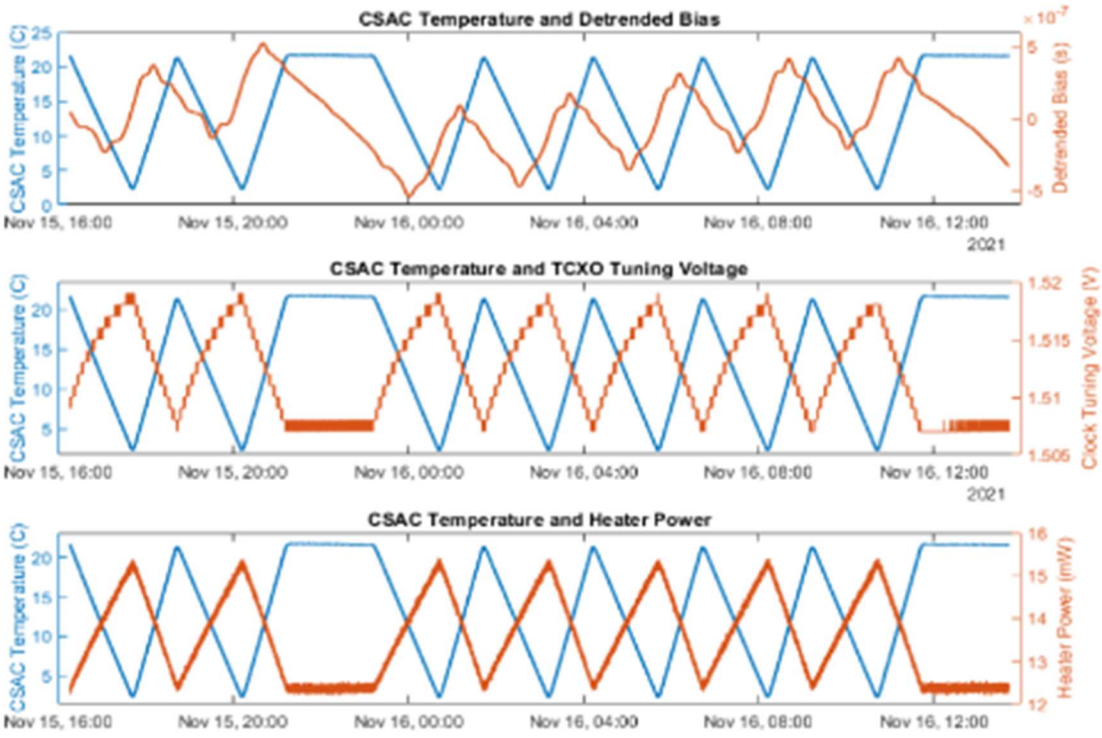

Figure 27. SpaceBuff detrended bias, temperature, tuning voltage, and heater power over time from Temperature Profile 3

LEO Temperature Profile 4

A similar test was performed using Ralphie, now at a higher temperature range and two thermal soak periods shown in Figure 28. However, during this test, the CSAC did not respond to temperature changes in the same manner as seen in previous tests. During the first two thermal cycles, Ralphie displays cyclical trends in the detrended clock bias as seen in other tests. In addition, during its two soaks, the clock bias trends linearly. This test further demonstrates that clock bias trends linearly while temperature is held constant and that the CSAC responds to heating and cooling in the temperature chamber.

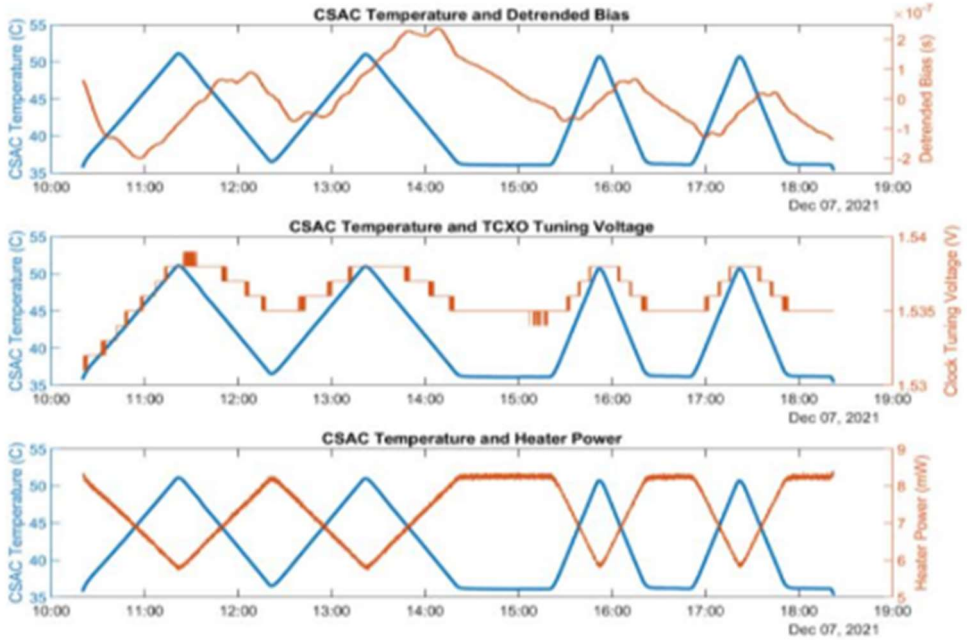

Figure 28. Ralphie detrended bias, temperature, tuning voltage, and heater power over time from Temperature Profile 4

4.2.4 CSAC Temperature Calibration Results

CSACs Chip and Ralphie were tested under a similar temperature profile as shown in Figure 4, with 30-minute ramp up/down periods, and 90-minute soak periods with increments of 10ºC. Unlike what is shown by MicroChip, these tests only have one cycle, rather than multiple, due to time constraints. Figure 29 and Figure 30 report the results of the two CSAC thermal tests.

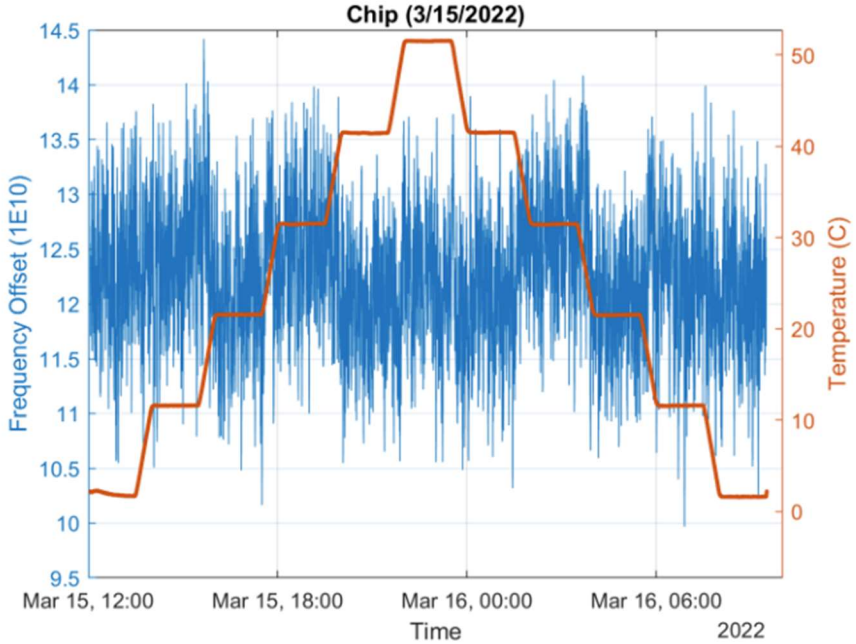

Figure 29. Chip 03/15/2022 - testing with MicroChip temperature profile

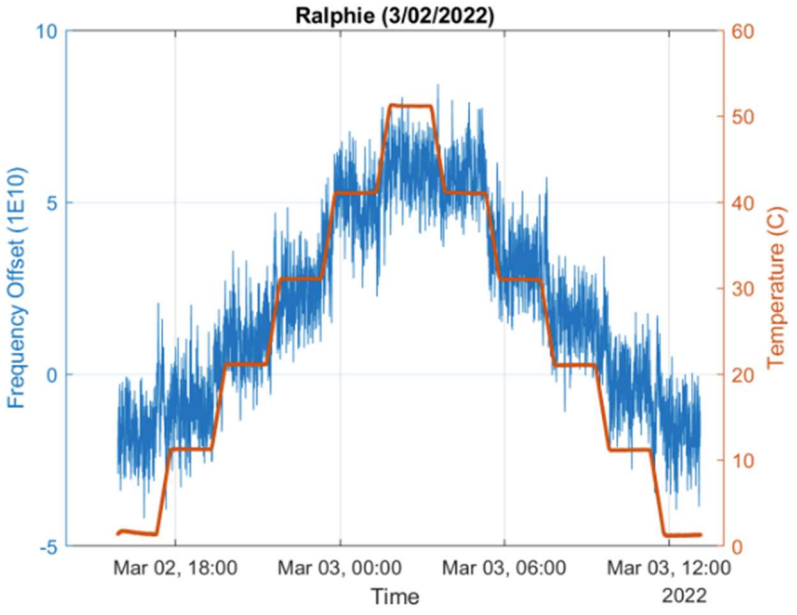

Figure 30. Ralphie 03/02/2022 - testing with MicroChip temperature profile

Figure 29 shows that the CSAC Chip, which is our most stable CSAC, performs as expected when compared to results from MicroChip. The frequency offset stays nearly centered and does not show significant changes due to thermal changes. On the other hand, Figure 30 shows that the temperature compensation on Ralphie is not tuned as well. The frequency offset increases and decreases with the temperature changes. After sharing these results with MicroChip, the CONTACT team was notified that it is likely that our clock has fallen out of specification during the time since being shipped to our lab (a time which exceeds the warrantee period).

4.2.5 Magnetic Field Testing Results

The measured magnetic fields for each torque rod are overlaid in Figure 31. Each test began with zero voltage applied to the torque rods, however, there is still a measured magnetic field. This offset is due to the Earth's magnetic field in Boulder.

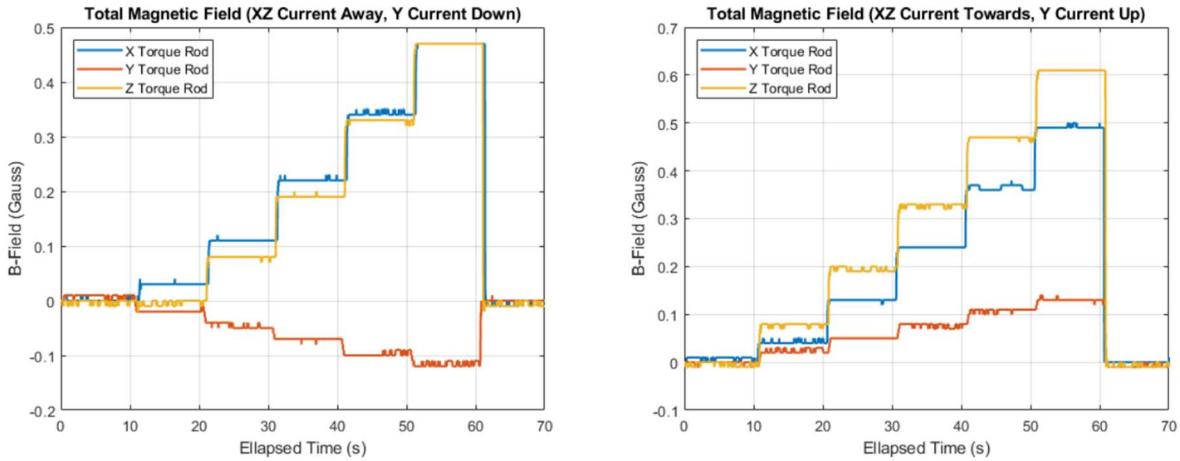

Figure 31. Overlaid magnetic field tests for individual torque rods

In both test cases, the Z torque rod resulted in the largest B-field, with the greatest magnitude in the "current towards" configuration. This is as expected because the Z torque rod is closest to the CSAC in the current MAXWELL configuration shown in Figure 5. The maximum magnetic field from each of these tests never exceeded 1 Gauss, indicating that the CSAC is not expected to be damaged by normal toque rod operations in flight. Following the individual torque rod tests, it was important to check that the combined magnetic field from all three torque rods in their worst-case scenario is still within the 2 Gauss specification from the manufacturer. Therefore, the test shown in Figure 31 was repeated, now with all three torque rods powered at the same time rather than individually. The results of this test are shown in Figure 32.

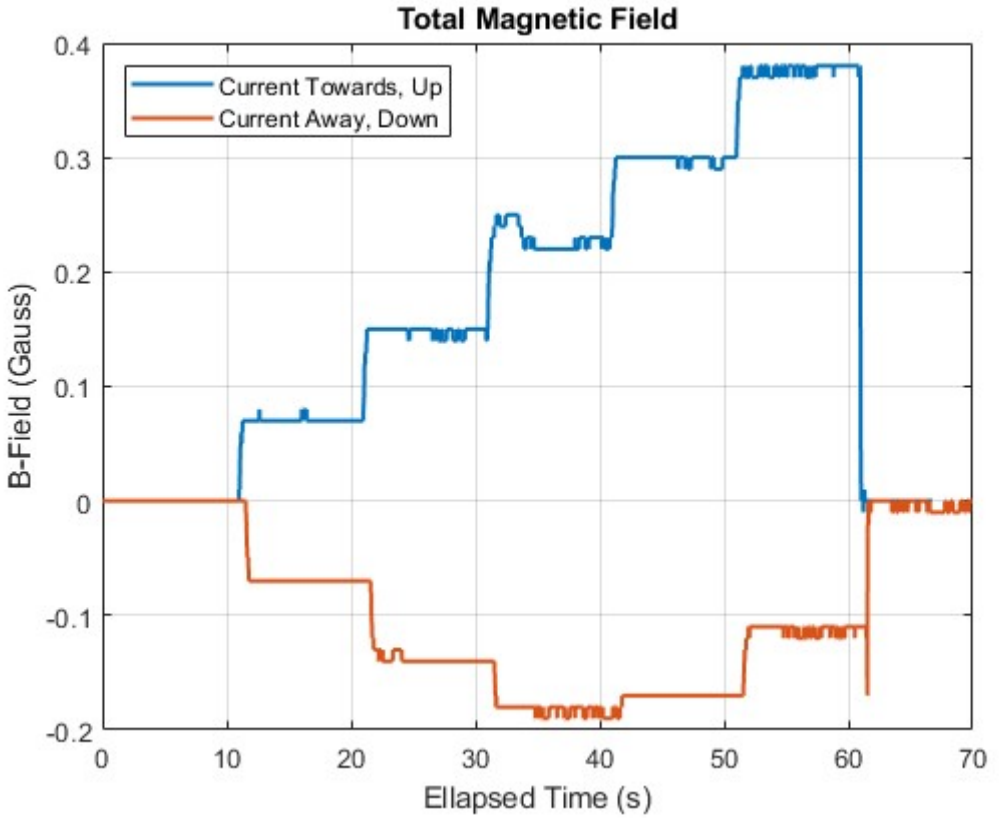

Figure 32. Total magnetic field (all torque rods)

The "current towards" configuration, shown in red, creates the largest B-field. However, because the B-field never reaches 0.7 Gauss, it indicates that the magnetic field produced by all three torque rods is not large enough to damage the CSAC.

The next magnetic field test was done with the nearest torque-rod and CSAC, as shown in Figure 6. The results from these tests are shown in Figure 33 and Figure 34.

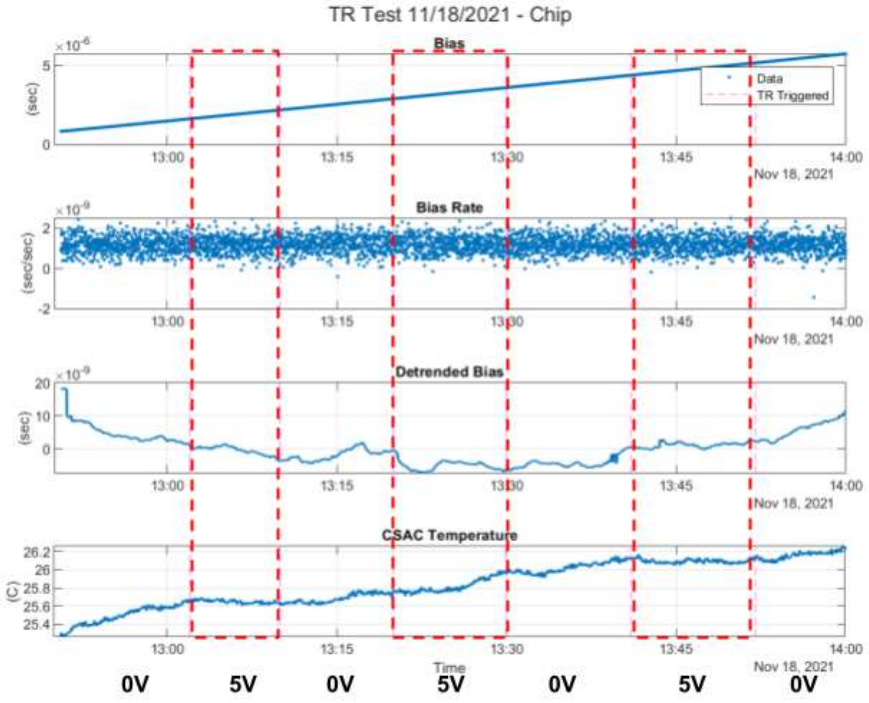

Figure 33. CSAC B-field sensitivity test 1

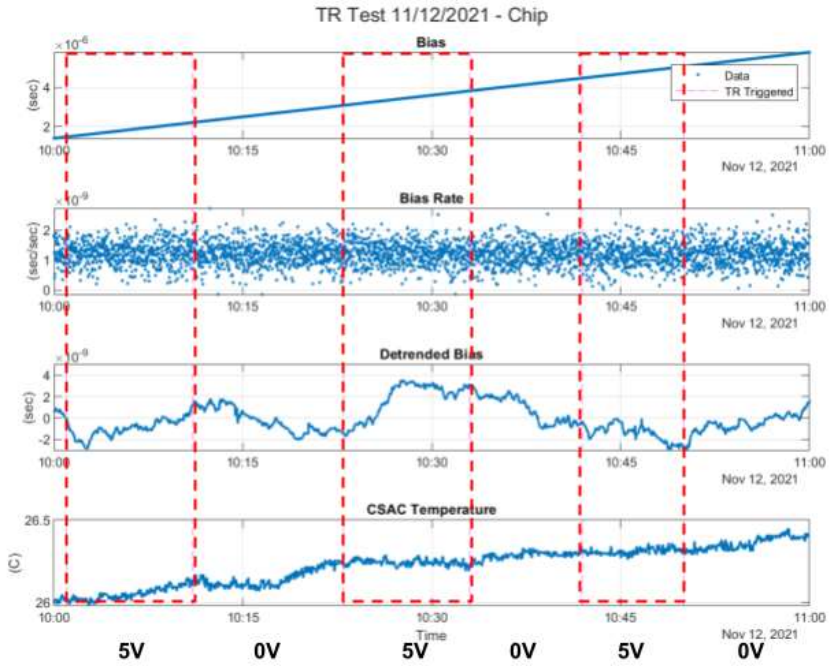

Figure 34. CSAC B-field sensitivity test 2

We found no evidence of a measurable impact caused by the torque rods. While the CSAC frequency may still be slightly altered by the magnetic field, our current measurement methods do not provide enough resolution to identify this. The CSAC and torque rod test can be repeated

using the SDR in order to eliminate the noise in the system introduced by GPS measuring approach. This may allow us to see finer frequency changes caused by the magnetic field. Additionally, the CSAC can be moved so that it experiences a stronger magnetic field. This would help us understand how the CSAC will behaves when magnetic fields are strong enough to significantly impact clock frequency. Nonetheless, we do not anticipate the CSAC data be impacted by the torque rod operation while on-orbit.

4.3 RF/GNSS Simulator Testing Results

4.3.1 Locked Clock Testing Results

The locked-clock tests were successful in verifying that the simulator can lock to the CSAC and rubidium as external references. Figure 35 shows a time series of the bias, bias-rate, and detrended bias from three separate tests in which the simulator, CSAC, and Rb were used to drive the simulator and GPS receiver clocks. The CSAC appears to wander more than the Rb and simulator clocks. Since the magnitudes of the bias and bias-rate are very small, we can conclude that the simulator is properly locking to the external reference.

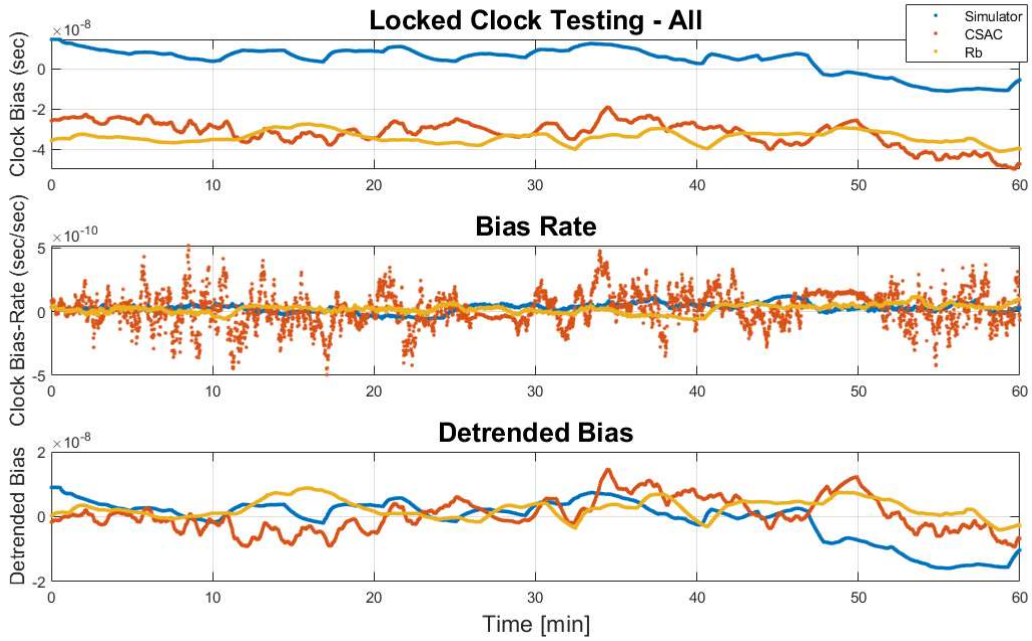

Figure 35. Locked-clock testing using the CSAC, Rb, and Spirent simulator as external reference to GPS receiver and Spirent simulator

4.3.2 Flight Mode Testing Results

The flight mode and locked-clock ADEV are shown in Figure 36. The flight mode ADEV is very different from what we observed in the live sky tests using the CSACs and the Rb. However, this behavior is like the ADEV plots from the locked-clock tests using the same LEO simulation.

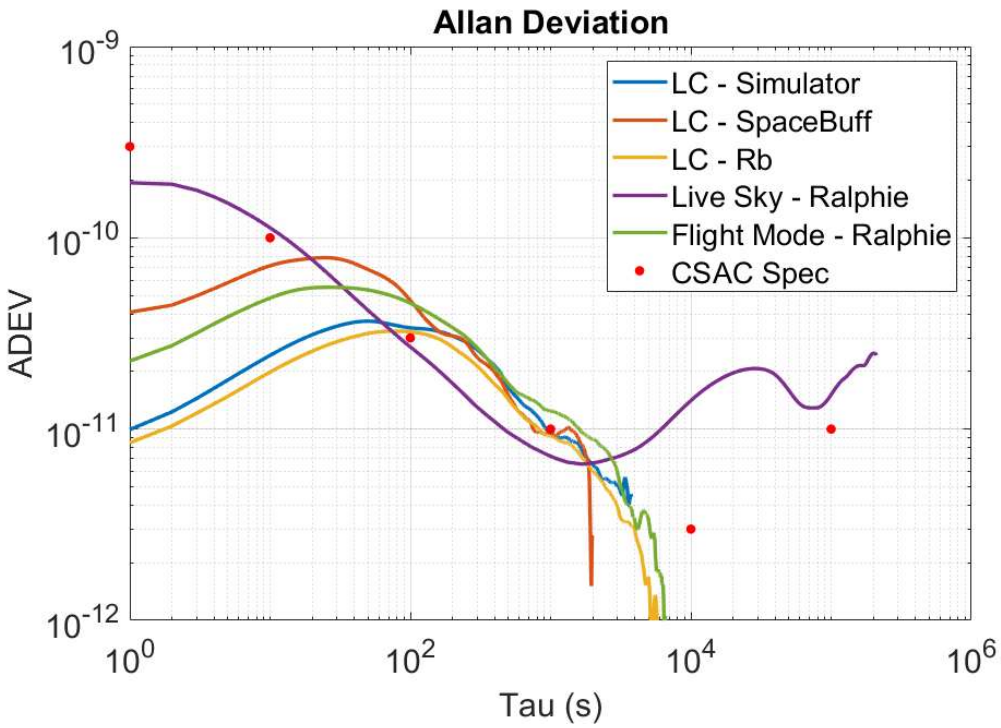

Figure 36. ADEV using receiver estimated clock bias from locked-clock, flight mode, and live sky tests

The low ADEV at 1 second and increase to a peak near 100 seconds time constant was unexpected. One candidate hypothesis for the cause of the large periodic effect on the clock bias, is an unmodeled or mismodeled, simulated relativistic effect on the receiver clock. Looking at the simulation parameters, we found that the orbital eccentricity is set to zero such that there should be no oscillation in the bias due to relativistic effects. An offset in the frequency due to the balance between special and general relativistic effects at the simulated receiver altitude should be present. However, in a live-sky test, this effect would be indistinguishable from a simple offset. In fact, both represent actual frequency efforts of the clock, so this effect is not one to be removed.

4.4 MAXWELL Integration & Testing Results

4.4.1 Hardware Testing Results

Live-sky testing on the EDU CSAC showed the CSAC “break-in” period, becoming more stable after being used for an extended period. The EDU CSAC is most like the CSAC that will be flown on-board MAXWELL. The main difference between this CSAC and ones typically tested is that the EDU is "space-rated" which simply means that it has under-gone testing under tighter constraints than the CSACs that have been tested with previously. The space rated CSAC should have consistent calibration to thermal changes and should ideally be more stable than our other clocks. The EDU CSAC was tested for 24 hours each on two different days, March 1st and March 9th. The CSAC was more stable on March 9th, than it was when first tested on March 1st. The stability of the clock can be seen in an ADEV Plot. Also, the plot of the CSAC’s detrended bias over time shows a steep decline in the first few hours of testing, and this curve characteristic

is not present in the second test. Prior to launch, the flight CSAC will be powered for a long duration test to allow it to “break in”.

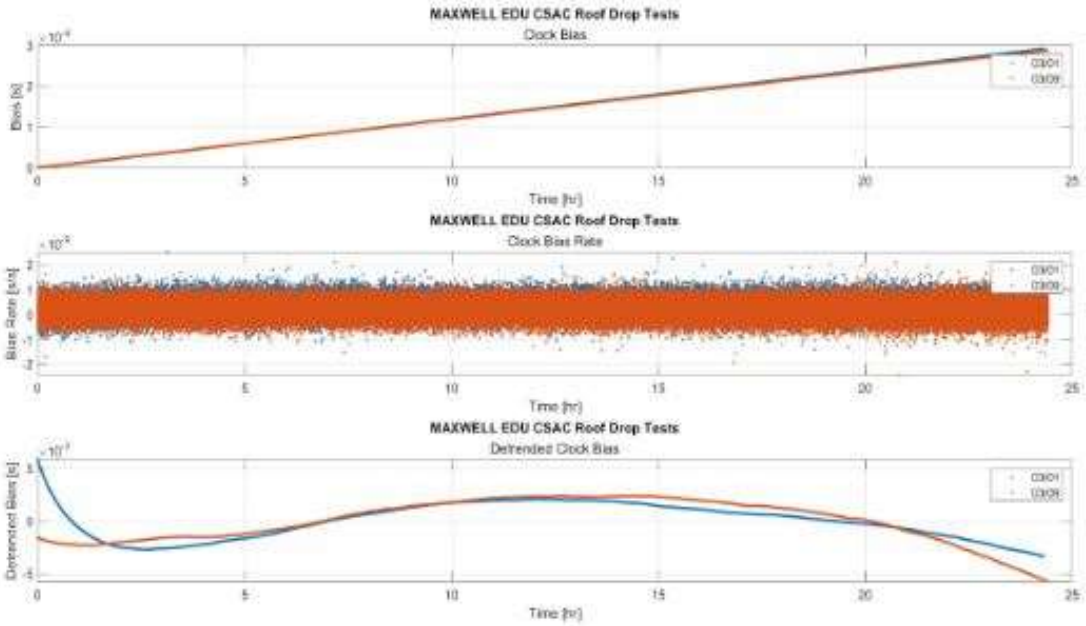

Figure 37. Time history plot of MAXWELL EDU CSAC live-sky test “break-in” period in clock bias-rate and detrended bias

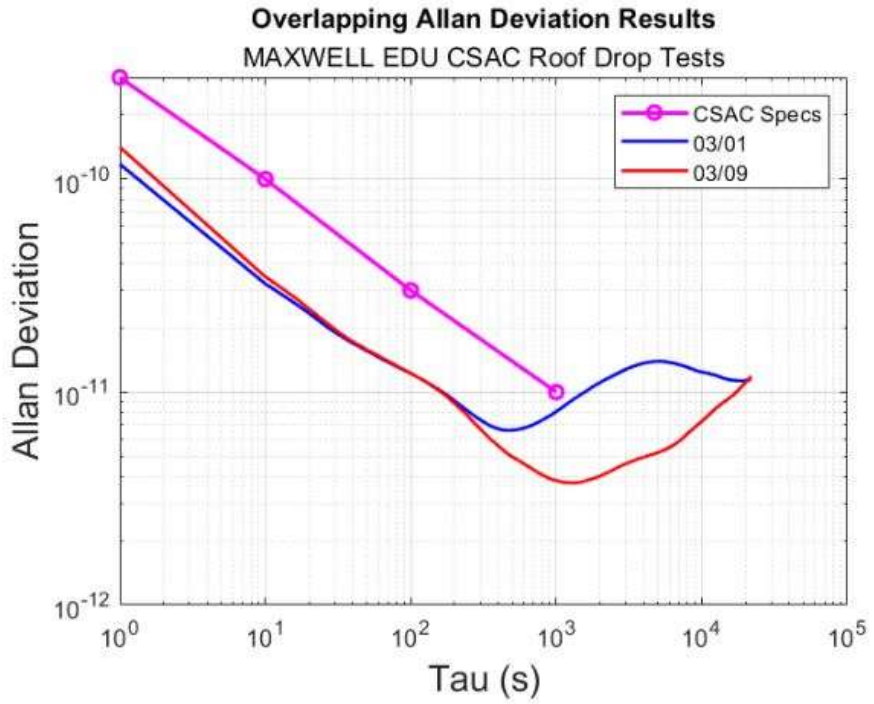

Figure 38. ADEV plot of MAXWELL EDU CSAC live-sky test "break-in" period

4.5 On-Orbit GPS Visibility Discussion

The CONTACT team has been working closely with MAXWELL to optimize GPS visibility during the CSAC experiment given MAXWELL power constraints. In order to have the best GPS satellite visibility on-orbit, the MAXWELL CubeSat's GPS antenna needs to be zenith pointing. However, due to the CubeSat's configuration and power requirements, it is unable to maintain a zenith point mode for an extended period (>4 hours) while remaining power positive. As such, the CubeSat will need to cycle between Sun and zenith point modes in order to re-charge during the CSAC experiment. This may negatively impact the GPS visibility during the experiment. To mitigate this risk, the entire telemetry data from the clock as well as full GPS messages will be collected during the experiment. Notably, pseudorange and range-rate data will be collected to assist with the limited GPS visibility. The CONTACT team intends to further address the impact of the lack of GPS visibility in simulation, as well as testing the orbit using the GNSS simulator with the NovAtel receiver.

4.6 Software Development & Testing

Lastly, efforts have been made to ensure proper software integration with the main MAXWELL flight loop. The MAXWELL team is still working on their main flight software loop, so full integration is not possible yet. However, the CONTACT team identified completed data-logging code for the flight CSAC drafted by CONTACT students in the past and the MAXWELL team is working to verify these data-logging tests are operable.

5. CONCLUSIONS

We look forward to finalizing plans for launch and finding resources to support operators and analysis for the flight experiment.

REFERENCES

[1] "MAXWELL - University Nanosatellite Program," [Online], available: https://www.colorado.edu/project/maxwellcubesat/our-mission.

[2] A. Aboaf, "MAXWELL Mission Handbook," 8 May 2020, [Online], available: https://drive.google.com/file/d/1T7kUrAEUulwJxJCrwVGooyidulDczV7b/view.

[3] Microchip, "Chip-Scale Atomic Clock (CSAC) SA.45 User's Guide," 2020, [Online], available: https://www.microsemi.com/document-portal/doc_download/135659-sa-45s-csac-user-guide.

[4] MicroChip, "SA.45s CSAC Data Sheet," [Online], available: https://ww1.microchip.com/downloads/en/DeviceDoc/00002985.pdf.

[5] NovAtel, "OEM7 Commands and Logs Reference Manual," April 2022, [Online], available: https://docs.novatel.com/OEM7/Content/PDFs/OEM7_Commands_Logs_Manual.pdf.

[6] Y. Khatri, A. Aboaf, D. Dowd, C. Flood, H. Dixon, and P. Axelrad, "CSAC Flight Experiment to Characterize On-Orbit Performance," Proceedings of the AIAA/USU Conference on Small Satellites, SSC20-XIII-03, https://digitalcommons.usu.edu/smallsat/2020/all2020/46/, August 2020.

[7] L. Schement and C. Dixon, "Ground Testing of a Chip-Scale Atomic Clock for MAXWELL CubeSat Flight Experiment," Proceedings of the AIAA/USU Conference on Small Satellites, SSC21-XIV-xx, https://digitalcommons.usu.edu/smallsat/2021/all2021/273 , August 2021.

[8] Dobbin, M., C. Colpaert, C. Krebs, and P. Axelrad, "Characterizing CSAC Performance in a Simulated Mission Environment," Proceedings of the 44nd Annual AAS Rocky Mountain Section Guidance, Navigation, and Control Conference 2022, Advances in the Astronautical Sciences, Breckenridge, CO, AAS 22-013, February 2022.

[9] W. Bertiger, Y. Bar-Sever, A. Dorsey, B. Haines, N. Harvey, D. Hemberger and P. Willis, "GipsyX/RTGx, a new tool set for space geodetic operations and research," *Advances in Space Research,* vol. 66(3), pp. 469-489, 2020.

[10] T. Yunck, T., "Coping with the Atmosphere and Ionosphere in Precise Satellite and Ground Positioning," In: Valance-Jones A (ed) *Environmental effects on spacecraft trajectories and positioning*. Washington: AGU Monograph. doi:10.1029/GM073p0001, 1993.

[11] J. Mason, B. Lamprecht, T. Woods and C. Downs, "CubeSat On-Orbit Temperature Comparison to Thermal-Balance-Tuned-Model Predictions," *Journal of Thermophysics and Heat Transfer,* vol. 32, no. 1, 2018.

[12] R. Lutwak, "Symmetricom - Technology Realization," *IEEE Frequency Control Symposium,* 2003.

DISTRIBUTION LIST

DTIC/OCP
8725 John J. Kingman Rd, Suite 0944
Ft Belvoir, VA 22060-6218 1 cy

AFRL/RVIL
Kirtland AFB, NM 87117-5776 1 cy

Official Record Copy
AFRL/RVB/Dr. Spencer E. Olson 1 cy

This page is intentionally left blank.